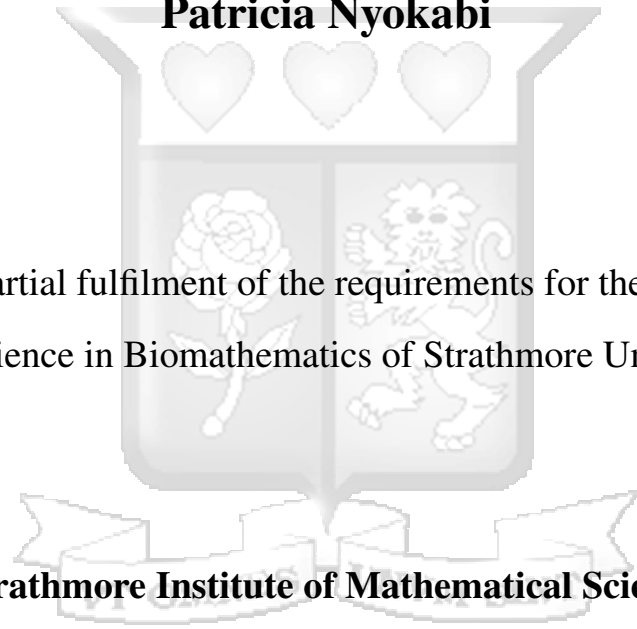


**Modeling Cholera Dynamics in Kenyan Slums: A
Comprehensive Analysis Incorporating WASH
Interventions, Vaccination, and Treatment**

Patricia Nyokabi

Submitted in partial fulfilment of the requirements for the degree of Master
of Science in Biomathematics of Strathmore University



**Strathmore Institute of Mathematical Sciences
Strathmore University
Nairobi, Kenya**

June 2025

This thesis is available for Library use through open access on the understanding that it is copyright material and that no quotation from the thesis may be published without proper acknowledgement.

Declaration

I declare that this work has not been previously submitted and approved for award of a degree by this or any other University. To the best of my knowledge and belief, the thesis contains no material previously published or written by another person except where due reference is made in the thesis itself.

© No part of this thesis may be reproduced without the permission of the author and Strathmore University.

Name: **Patricia Nyokabi**

Signature: 

Date: **May 22, 2025**

Approval

The thesis of Patricia Nyokabi has been reviewed and approved by the following:

Dr. Titus Orwa

Supervisor,

Lecturer, Strathmore Institute of Mathematical Sciences.

Prof. Rachel Waema

Supervisor,

Professor, Strathmore Institute of Mathematical Sciences.

Dr. Godfrey Madigu

Dean, Strathmore Institute of Mathematical Sciences,

Strathmore University.

Prof. Bernard Shibwabo

Director of Graduate Studies,

Strathmore University.

Abstract

Cholera is an acute intestinal disease which has become a global public health concern, especially in regions where water, sanitation and hygiene (WASH) amenities are inadequate. In the period from January - September 2024, Africa reported 127283 cases, with 2268 deaths. In Kenya, cholera has been reported especially in areas with inadequate access to safe water and proper hygienic facilities such as urban informal settlements, large refugee camps, pastoral areas, arid and semi arid lands, areas bordering water bodies and Mwea irrigation scheme. By developing a deterministic mathematical model, this study determined the effectiveness of various WASH interventions in preventing and eradicating cholera in Nairobi slums. The system of ODE's and the optimal control model were solved numerically using the Runge-Kutta fourth-order method implemented in R, with the forward-backward sweep method applied for the optimal control problem. Scenario analysis was applied to assess the impact of different strategies for controlling the spread of cholera. Results revealed that an integration of all control strategies was necessary and prioritizing water treatment, sanitation, and hygiene promotion can yield substantial public health benefits. The numerical simulations showed that if only one WASH intervention is feasible, improved sanitation and safe fecal sludge management, or water treatment should be prioritized. If two interventions can be implemented, water treatment and waste management should be preferred, followed by hand hygiene and hygienic practices in food handling with sanitation infrastructure. If resources accede three WASH interventions, priority should be given to water treatment, improved sanitation and waste management. The results obtained will provide valuable insights on improvements and steps to take for development of better strategies in management of cholera spread.

Table of contents

List of figures	vi
List of tables	ix
List of Abbreviations	x
Acknowledgement	xi
1 Introduction	1
1.1 Background to the Study	1
1.1.1 Cholera	1
1.1.2 Water Sanitation and Hygiene (WASH)	4
1.1.3 Vaccination	5
1.1.4 Treatment	6
1.2 Statement of the Problem	7
1.3 Research Objectives	8
1.3.1 General Objective	8
1.3.2 Specific Objectives	8
1.4 Scope of the Study	8
1.5 Significance of the Study	9
2 Literature Review	10
2.1 Introduction	10
2.2 Cholera Models	10
2.2.1 Research Gap	14

3	Methodology	15
3.1	Model Formulation	15
3.1.1	Compartmental Model	17
3.1.2	Model Equations	19
3.2	Model properties	19
3.2.1	Positivity of Solutions	19
3.2.2	Boundedness of Solutions	21
3.3	Equilibria Points and Stability Analysis	24
3.3.1	Disease Free Equilibrium Point	24
3.3.2	Effective Reproduction Number	24
3.3.3	Local Stability of Disease Free Equilibrium	27
3.3.4	Global Stability of Disease Free Equilibrium	29
3.4	Sensitivity Analysis	31
3.5	Optimal Control Analysis of WASH Interventions	34
4	Results and Discussion	38
4.1	Scenario Analysis of the Impact of Control Strategies	38
4.1.1	Impact of Interventions on Treated Cases	38
4.1.2	Impact of Interventions on Untreated Treated Cases	40
4.1.3	Impact of intervention strategies on bacterial density	41
4.1.4	Temporal Dynamics of Combined Cholera Interventions	42
4.2	Optimal Control Analysis of WASH Interventions	43
4.2.1	Impact of Individual WASH Intervention	43
4.2.2	Effects of Two Distinct Combined WASH Interventions	48
4.2.3	Impact of Three Different Combined WASH Interventions	51
5	Conclusion and Recommendation	55
5.1	Conclusion and Recommendation	55
	References	58
	Appendices	62

List of figures

Figure 3.1: Cholera dynamics conceptual model. See Equation (3.1) for definition of Λ	17
Figure 4.1: Impact of intervention strategies on T_i	39
Figure 4.2: Impact of intervention strategies on I_n	41
Figure 4.3: Impact of intervention strategies on B	42
Figure 4.4: Impact of individual WASH intervention on T_i . The control parameters ω_1 to ω_4 represent reduction of environmental contamination, reduction of human-to-human transmission, reduction of pathogen shedding by infected individuals, and acceleration of environmental pathogen decay, respectively. Each subplot compares the intervention scenario to the no-intervention baseline.	45
Figure 4.5: Impact of individual WASH intervention on I_n . The control parameters ω_1 to ω_4 represent reduction of environmental contamination, reduction of human-to-human transmission, reduction of pathogen shedding by infected individuals, and acceleration of environmental pathogen decay, respectively. Each subplot compares the intervention scenario to the no-intervention baseline.	46
Figure 4.6: Impact of individual WASH intervention on B . The control parameters ω_1 to ω_4 represent reduction of environmental contamination, reduction of human-to-human transmission, reduction of pathogen shedding by infected individuals, and acceleration of environmental pathogen decay, respectively. Each subplot compares the intervention scenario to the no-intervention baseline.	47

Figure 4.7: Impact of 2 WASH interventions on T_i . The control parameters ω_1 to ω_4 represent reduction of environmental contamination, reduction of human-to-human transmission, reduction of pathogen shedding by infected individuals, and acceleration of environmental pathogen decay, respectively. Each subplot compares the intervention scenario to the no-intervention baseline.	49
Figure 4.8: Impact of 2 WASH interventions on I_n . The control parameters ω_1 to ω_4 represent reduction of environmental contamination, reduction of human-to-human transmission, reduction of pathogen shedding by infected individuals, and acceleration of environmental pathogen decay, respectively. Each subplot compares the intervention scenario to the no-intervention baseline.	50
Figure 4.9: Impact of 2 WASH interventions on B . The control parameters ω_1 to ω_4 represent reduction of environmental contamination, reduction of human-to-human transmission, reduction of pathogen shedding by infected individuals, and acceleration of environmental pathogen decay, respectively. Each subplot compares the intervention scenario to the no-intervention baseline.	51
Figure 4.10: Impact of different WASH interventions on T_i . The control parameters ω_1 to ω_4 represent reduction of environmental contamination, reduction of human-to-human transmission, reduction of pathogen shedding by infected individuals, and acceleration of environmental pathogen decay, respectively. Each subplot compares the intervention scenario to the no-intervention baseline.	52
Figure 4.11: Impact of different WASH interventions on I_n . The control parameters ω_1 to ω_4 represent reduction of environmental contamination, reduction of human-to-human transmission, reduction of pathogen shedding by infected individuals, and acceleration of environmental pathogen decay, respectively. Each subplot compares the intervention scenario to the no-intervention baseline.	53

Figure 4.12: Impact of different WASH interventions on B . The control parameters ω_1 to ω_4 represent reduction of environmental contamination, reduction of human-to-human transmission, reduction of pathogen shedding by infected individuals, and acceleration of environmental pathogen decay, respectively. Each subplot compares the intervention scenario to the no-intervention baseline. 54



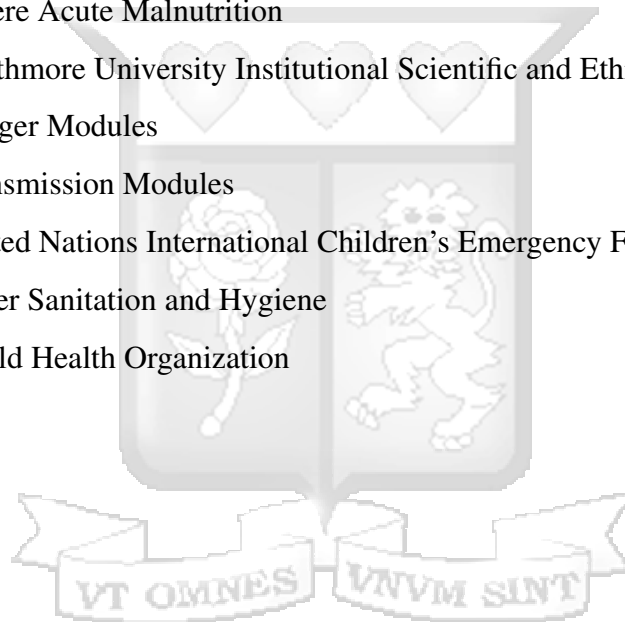
List of tables

Table 3.1: Model parameters	18
Table 3.2: Parameter values	33
Table 3.3: Sensitivity indices (SI)	34



List of Abbreviations

AMR	Antimicrobial Resistance
GAVI	Global Alliance for Vaccines and Immunization
MCMC	Markov Chain Monte Carlo
MoH	Ministry of Health
OCV	Oral Cholera Vaccine
ORS	Oral Rehydration Solution
SAM	Severe Acute Malnutrition
SU-ISERC	Strathmore University Institutional Scientific and Ethics Review Committee
TM	Trigger Modules
TrM	Transmission Modules
UNICEF	United Nations International Children's Emergency Fund
WASH	Water Sanitation and Hygiene
WHO	World Health Organization



Acknowledgement

I thank God Almighty for giving me good health, wisdom, and perseverance throughout this research journey. His grace has illuminated my path and this achievement would not have been possible without Him.

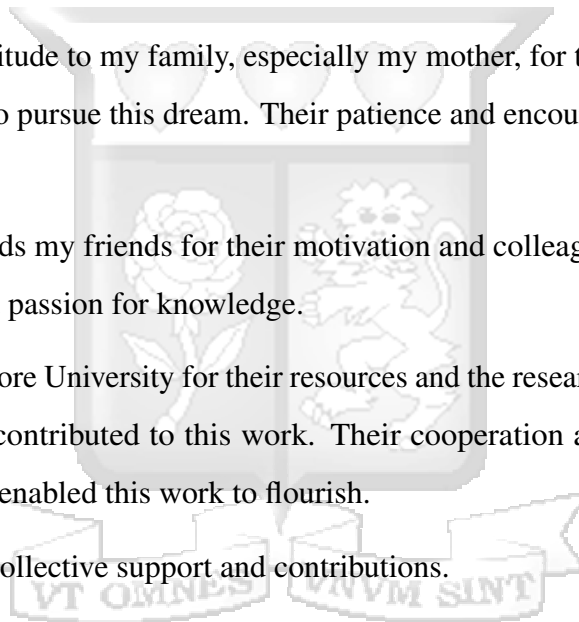
I would also like to express my sincere gratitude to my supervisors, Prof. Rachel Waema and Dr. Titus Orwa for their valuable guidance, constructive feedback and unwavering support. Their expertise and mentorship were fundamental in shaping this work.

I offer my deepest gratitude to my family, especially my mother, for their love and sacrifices that have enabled me to pursue this dream. Their patience and encouragement have kept me grounded.

My appreciation extends my friends for their motivation and colleagues for their insightful discussions and shared passion for knowledge.

I acknowledge Strathmore University for their resources and the research communities whose experiences and data contributed to this work. Their cooperation and insights have been instrumental and have enabled this work to flourish.

Thank you all for the collective support and contributions.



Chapter 1

Introduction

1.1 Background to the Study

1.1.1 Cholera

Throughout the world, there are about 1.3 to 4 million reported cases of cholera and 21,000 to 143,000 reported deaths per year due to cholera (Awofeso and Aldbak, 2018). 50% of the reported cases in the World Health Organization between 1980 and 2011 came from sub-Saharan Africa (Bwire et al., 2017) while between 2010 and 2019, the reported cases were 24% (Zheng et al., 2022). According to WHO, the official reported cases represent only 5-10% of the actual number occurring worldwide per year. In Kenya, over 25000 cholera cases were reported between 2015 and 2019 (Kiama et al., 2023). According to WHO, Kenya has been faced with mass outbreaks of cholera since 2014. In 2015, 10568 cases were reported, 5208 in 2019 and from October 2022 to October 2023, Kenya had reported 12120 cases, with 1.7% case fatality rate (Cheng, 2024). A study done to identify cholera hotspots in Kenya revealed that of the 290 sub-counties in the country, 25 (8.6%) were epidemiological priority; 78 (26.9%) WASH priority; and 30 (10.3%) were based on a combination of epidemiological and WASH indicators (Kiama et al., 2023).

Cholera is an acute intestinal disease transmitted by ingesting food or water contaminated with the bacteria *Vibrio cholerae*. It is characterized by vomiting, watery diarrhoea, leg cramps, restlessness, and irritability. Many serotypes of *Vibrio cholerae* have been identified based on the Somatic O antigen which determines the potential for bacterial pathogenicity. However, only the O1 and O139 serogroups are linked to the majority of cholera outbreaks (Abdulrahim and Adesola, 2022). When infection occurs, the bacterium passes through the

gastric acid barrier of the stomach, of which it survives, there after infiltrating the mucus coating of the epithelium in the human host's small intestine (Cui et al., 2014). After they populate the intestinal gut, they produce enterotoxin which acts on the mucosal epithelial cells (Kobe et al., 2018). This causes the symptoms that can lead to severe dehydration and death within three to four hours if untreated (Hartley et al., 2006). During shedding, *Vibrio cholerae* enters a brief hyperinfective state which causes infection even with asymptomatic carriers. Cholera has an incubation period of between 12 hours and 5 days after which symptoms begin to appear (Onuorah et al., 2022).

The main route for cholera transmission is the fecal-oral route (Abdulrahim and Adesola, 2022). Fecal-oral transmission occurs when bacteria from an infected stool of an individual contaminates water, food, hands, houseflies, or the soil, which later gets into the mouth of another individual either directly or indirectly. This introduces two pathways of cholera transmission. The environment-to-human transmission where bacteria is consumed directly from contaminated rivers or streams and human-to-human transmission where contaminated food by an infected person is ingested by a susceptible individual. Human-to-human transmission often occurs among household contacts with an infected case (Cui et al., 2014).

Cholera still is a global public health concern, particularly in areas where water, sanitation and hygiene (WASH) amenities are inadequate. These are areas affected by poverty, poor environmental conditions, or other humanitarian crises (Kobe et al., 2018). Cholera in Kenya has been reported especially in areas where poor and vulnerable communities live in informal settlements in urban areas and refugee camps, with inadequate access to safe water and proper hygienic facilities (Mageto et al., 2023). According to Kiama et al. (2023), urban informal settlements, large refugee camps, pastoral areas, arid and semi arid lands, areas bordering lake Victoria region and Mwea irrigation scheme are the major cholera hotspots in Kenya. Poor hygiene practices, inadequate safe water, insufficient toilet facilities and ineffective waste treatment significantly increase the risk of cholera outbreaks in informal settlements (Mageto et al., 2023). Rapid urbanization and economic factors are some of the determinants that lead to growth of these informal settlements. They are characterized by high population density, poor infrastructure and low access to social amenities.

The history of cholera cases in Nairobi indicate that cholera outbreaks mostly occurred in the central and eastern parts of Nairobi (Manaseh et al., 2023). The outbreaks trailed an East-West direction affecting areas like Kibera, Kangemi, Makadara and Embakasi. From the year 2009 to 2019, Embakasi area in Nairobi County was worse hit by cholera outbreaks. Embakasi is home to many slums including Kware, Korogocho, Pipeline, Mukuru, and Embakasi South and North. These are highly populated areas with dense housing environments, poor waste management, open sewage systems and dumping sites. According to Manaseh et al. (2023), historical data revealed cholera cases were connected to areas with low social-economic status where standard sanitation was lacking. These areas included slums in Kibera, Dagoretti North, Mathare, Kamukunji and all sub-counties in Embakasi. The spread of cholera was propagated by contaminated food and drinking water in eateries, accompanied by poor hygiene (Manaseh et al., 2023). Climatic changes such as rainfall, humidity and temperature also played a role in the history of cholera cases in Nairobi slums. These areas were likely to be contaminated during rainy seasons.

It is estimated that 60% of Nairobi's residents live in informal settlements, with Kibera being one of the largest among them. According to Kim et al. (2022), 77.4% of people living in Kibera have limited access to water, sanitation and hygiene. Another Nairobi slum, Mathare, has an average of five people living in a 12-square meter dwelling. According to Kamau and Njiru (2018), Mathare is not covered by the Nairobi Water and Sewerage Company. Residents pay 15.3 times the standard price for water. The authors further explain that expenditure on water is 20% their total income where generally, expenditure on water should not surpass 3%. Water is stored in wide-opened uncovered containers on the ground, from which it is drawn by dipping, and is mostly not treated. This increases the chance of contamination. In regards to defecation, Kamau and Njiru elucidates that 5% of Mathare households practice open defecation. "Flying toilets" are also common, where an individual defecates in a paper bag and throws it in the roof of the next house. Additionally, sanitation facilities are shared by approximately 65 people per facility, encouraging transmission of bacteria (Kamau and Njiru, 2018). In a humanitarian crisis, a maximum of 20 people per facility are the minimum standards prescribed. This suggests that the probability of refugee camps having more sanitation facilities is higher as compared to Mathare slums. Furthermore,

children's excreta are disposed to an open drain that empties to a river, where water vendors and food kiosk workers retrieve their water (Kamau and Njiru, 2018). The crucial moments to wash hands with soap and water in order to prevent diarrheal diseases are before eating, before preparing food, after defecation, after handling child's stool and before feeding a child. In Mathare, only 25% washes their hands during atleast three of these crucial moments. Of these, only 50% use soap (Kamau and Njiru, 2018). Access to safe water and sanitation is highly correlated with income and level of education, and it shows the contribution of social-economic principles on health of residents in informal settlements.

1.1.2 Water Sanitation and Hygiene (WASH)

WASH intervention primarily involves water quality, handwashing with soap and excreta disposal (Cairncross et al., 2010). If an outbreak arises, WHO provides a response to reduce mortality and morbidity. In the case of a cholera outbreak, recommendations on immediate management of infected cases and provision of safe water, improved hygiene and sanitation, safe standards on food handling are instructed (Taylor et al., 2015). Practices like application of chlorine in water stored in individual water containers, or water distributed in water trucks or delivering products for household water treatment are the first response to an outbreak. In addition to this, promotion of household disinfection, personal and food hygiene as well as distribution of hygiene kits constitute part of the WASH intervention applied (Taylor et al., 2015). According to Cairncross et al. (2010), intervention of handwashing with soap should be done after excretion or contact with child feces, before eating or preparing food, or mixture of these. Fecal disposal interventions aim to help manage human waste in a way that limits direct or indirect human interaction. Basic pit latrines, bucket toilets, hanging toilets, and composting toilets are all methods for containing human excreta and should be differentiated from open defecation. (Cairncross et al., 2010). Some of the challenges associated with implementing WASH in urban informal settlements include lack of sufficient water supply, inadequate wastewater management, poor personal hygiene, poor community hygiene and sanitation and poor maintained sewage facilities (Manaseh et al., 2023). Other factors related to safe water are unhygienic water vending facilities, lack of tap water in

households and limited water treatment. Although most households in the Nairobi informal settlements have access to flush toilets, they are illegally connected to the sewer lines ([Kamau and Njiru, 2018](#)).

1.1.3 Vaccination

Aside from WASH, Oral Cholera Vaccine (OCV) has been recommended in the fight against cholera. According to WHO standards, three OCV namely Dukoral, Shanchol, and Euvichol are pre-qualified ([Shaikh et al., 2020](#)). OCV offers immunity in adults and older children, and limited protection in children under the age of 5. The direct protection in conjunction with the herd immunity makes it cost effective and desirable in the developing countries. Due to WHO recommendation on usage of OCV, there has been global demand for it mainly driven by epidemics and outbreaks. Additionally, OCV vaccination campaigns, its availability and ease of use, demonstrated protection to vulnerable populations and GAVI (Vaccine Alliance) cooperation in vaccine costs, has increased the demand for OCVs ([Shaikh et al., 2020](#)).

In Kenya, the first cholera vaccine was introduced in February 2023, following a cholera outbreak in October 2022. Before that, the first cholera incidence was reported in 1971 followed by a series of identical outbreaks in the years 1997–1999, 2007–2010, 2015–2020 ([Anis et al., 2023](#)). During the outbreak in 2022, Nairobi’s informal settlements raised concerns due to clustered poor population with lack of sanitation services and reliable sewage management. According to [Cheng \(2024\)](#), there were at least 7,800 cases and 122 deaths across the country towards the end of March 2023, of which 1196 were from Nairobi. However, cholera vaccine campaigns had a positive impact on the outbreak. Most of the residents in the informal settlements in Nairobi got to be aware of the great risk they were in due to congestion and poor sanitation and consequently, vaccines were highly welcomed with no challenges.

1.1.4 Treatment

Therapy regarding cholera is based on successful replacement of the fluid and electrolytes lost from the gastrointestinal tract. This is achieved through oral rehydration solution (ORS), intravenous fluid therapy and oral electrolyte therapy. A WHO standard ORS sachet is dissolved in 1 litre of water, where adult patients can take up to 6 litres on the first day (WHO, 2023a). Success of intravenous fluid is characterized by solute concentrations of the fluid, route of administration and rate at which it is being administered, all depending on the degree of saline depletion (Bhattacharya, 2003). Oral electrolyte therapy involves uptake of sodium in conjunction with glucose. Glucose escalates absorption of sodium by the small intestine. When cholera infection occurs, the small intestine increasingly secretes isotonic fluids due to the cholera enterotoxin. Since the enterotoxin has no effect on glucose movement from gut to plasma, the solution containing glucose and sodium is orally administered to maintain adequate fluid and electrolyte balance (Carpenter, 1971).

In severely sick patients, and those with high purging or significant co-morbidities such as severe acute malnutrition (SAM) and pregnancy, recommended antibiotics (antimicrobials) are used to decrease the period and volume of diarrhoea and lessen the shedding of *V. cholerae* (GTFCC, 2018). Some of the antibiotics include tetracycline, norfloxacin, ciprofloxacin, furazidone and doxycycline (Chowdhury et al., 2022). The antibiotics target the bacterial 30S ribosomal subunits and protein synthesis (Abdulrahim and Adesola, 2022). It is recommended that the antibiotics are taken in conjunction with the rehydration therapy. Resistance of antimicrobial (AMR) has also become a matter of concern. The mass administration (WHO, 2023a) and overuse (GTFCC, 2018) of antibiotics in patients that are less probable to clinically benefit has contributed to AMR. Most *V. cholerae* are resistant to chloramphenicol, co-trimoxazole and furazolidone which are consequently no longer used (GTFCC, 2018). According to Abera et al. (2010), *V. cholerae* O1 serotype are resistant to co-trimoxazole, chloramphenicol, ampicillin, and tetracycline. In children under the age of 5, zinc supplements are used to reduce the severity of diarrhoea. It regenerates the intestinal epithelium and increases the absorption of water and electrolytes (Chowdhury et al., 2022).

1.2 Statement of the Problem

About 4 million cases of cholera and 143,000 cholera deaths are reported annually throughout the world. The actual number is possibly significantly higher, as numerous cases remain unreported, particularly in developing countries in sub-Saharan Africa where it is still endemic. Cholera continues to pose a serious public health problem majorly in the vulnerable population where safe water and sanitation resources are limited. In Kenya, the major cholera hotspots are urban informal settlements, large refugee camps, pastoral areas, arid and semi arid lands, areas bordering lake Victoria region and Mwea irrigation scheme (Kiama et al., 2023). Manaseh et al. (2023) indicated that cholera outbreaks were more prevalent in central and eastern parts of Nairobi, which hosts the most of the slums. The slum areas are characterized by lack of sufficient water supply resulting to unhygienic water vending facilities, inadequate wastewater management, poor personal hygiene, poor community hygiene and sanitation and poorly maintained sewage facilities. Subject to this, the transmission of cholera through the fecal-oral route is propagated. Moreover, suitable conditions are created for the bacteria *V. cholerae* to thrive with an increasing rate and intensity.

Conventional interventions like emergency treatment and retaliatory vaccination campaigns have proved not effective enough for preventing the spread of cholera in these communities. Different strategies are required for different locations (slums) and should be put in place in order to effectively combat cholera infection. Mathematical models in literature have minimal consideration of how various factors contribute to the spread of the disease, limiting the ability to accurately assess the impacts of WASH facilities with treatment and vaccination. A holistic understanding of how human practices and environmental contamination connect with public health interventions to affect the spread of the disease is required. This research aims to address these complex dynamics of cholera transmission and identify the most effective combination of intervention strategies.

1.3 Research Objectives

1.3.1 General Objective

To develop a mathematical model for cholera that incorporates WASH, treatment and vaccination as interventions.

1.3.2 Specific Objectives

1. To develop a mathematical model for cholera infection that incorporates WASH interventions.
2. To assess the effect of enhanced WASH, vaccination and treatment on cholera dynamics through scenario analysis.
3. To identify the most effective combination of WASH interventions, for managing cholera infections in Nairobi slums through optimal control analysis.

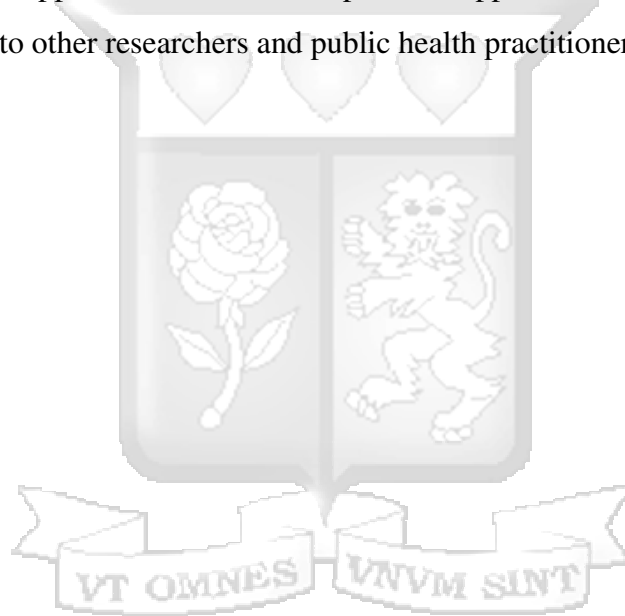
1.4 Scope of the Study

A deterministic mathematical model described by a system of ordinary differential equations, is used to simulate different levels of WASH interventions as well as vaccination and treatment. The next generation matrix approach is used to determine the effective reproduction number R_v , and consequently, the stability of the disease free equilibrium. The study focuses on the informal settlements of Nairobi County in Kenya that have limited access to safe water and sanitation. Secondary data from published research is used to develop and analyze the proposed model. Parameter estimates for the model were drawn from previously published scholar sources and reports from credible organizations such as WHO. In pursuance of relevance of parameters, preference was given to studies conducted in similar geographic and socioeconomic contexts. The study does not cover the seasonal and climatic variation that influence pathogen concentration.

1.5 Significance of the Study

Incorporation of WASH, vaccination, treatment and direct and indirect transmission in the model will enable more accurate design of effective, targeted control programs. This means that the results obtained from this study will inform decision making and provide proof to support policies that stress on sustainable intervention programs in settings of limited resources.

By focusing specifically on Nairobi slums, the mathematical model ensures a practical and customized applicability thereby filling a gap existing in literature. In addition, the research produces a modified approach that can be adapted and applied to other infectious diseases, making it valuable to other researchers and public health practitioners in general.



Chapter 2

Literature Review

2.1 Introduction

Cholera being a significant public health challenge, a comprehensive investigation of its etiology, pathophysiology, and control measures in order to help form effective prevention and treatment strategies is necessary. Mathematical models provide valuable insights into the transmission dynamics, and provide guidance on optimal control strategies ([Tuite et al., 2011](#)). Over the years, a number of mathematical models have been developed and used to study the dynamics of cholera spread.

2.2 Cholera Models

In a study done by [Tuite et al. \(2011\)](#), a cholera transmission model was used to predict the sequence and timing of regional cholera epidemics in Haiti and explore the potential effects of disease-control strategies. The authors developed a compartmental mathematical model that allowed person-to-person and waterborne transmission of cholera which modelled within- and between-region epidemic spread. Their results showed a basic reproduction number ranging from 2.06 to 2.78. They found that the order and timing of regional cholera outbreaks were associated with empirical observations. Additionally, the authors claimed that the limited use of vaccines that were supplied late in the epidemic would have a modest effect.

[Ayoade et al. \(2018\)](#), incorporated preventive and control measures as well as person-to-person disease transmission into [Fung \(2014\)](#)'s model, which only involved environment-to-human transmission. The equilibrium analysis showed the existence of disease free

equilibrium and endemic equilibrium, which were locally asymptotically stable when the basic reproduction number was less than unity. The results of their analysis indicated that in order to curb cholera outbreak effectively, a wide coverage of cholera vaccination and drug treatment in cholera endemic regions is essential. The authors claimed that the accessibility and potency of these interventions can deter 120,000 deaths caused by cholera annually. Similarly, [Cui et al. \(2014\)](#), developed a mathematical model for cholera that integrated a vaccination compartment. Analysis revealed that cholera can be eliminated from the community if vaccines, although imperfect, brings R_v to a value less than unity. The authors also illustrated that the vaccine would always reduce the reproduction number of cholera, and in its absence, the disease transmission would be high.

In contrast, a model fitted to Uganda cholera cases between 1999 to 2015 showed that the suitability of vaccination in combating cholera was not as great as controlling over the long and short cycle transmission route ([Onuorah et al., 2022](#)). [Onuorah et al. \(2022\)](#), developed a Susceptible-Infected-Recovered-Bacteria (SIRB) deterministic model that considered immigration in the dynamics of cholera transmission. Aside from control over long and short transmission cycle being a better strategy than vaccination in the fight against cholera in Uganda, their findings further suggested a correlation between the number of infected immigrants and the number of infected individuals in the population. This confirmed the contribution of immigration in the spread of cholera in Uganda. In China, improved environmental sanitation and availability of clean water is a better strategy when compared to vaccination ([Sun et al., 2017](#)).

A study done by [Kobe et al. \(2018\)](#), considered the aspect of priority in individual participation in interventions against cholera. A game-theoretic model was constructed to determine the effect of personal amenability in deciding which intervention program to participate in, either vaccination or clean water consumption, under assumed costs. The study revealed that voluntary participation in those policies reached levels close to those required for herd immunity and cholera incidence could be reduced as long as the relative costs of the interventions remained low. If a certain threshold level was exceeded, then the intervention would be non-viable since individuals would rather risk infection than take costly protective measures.

The authors findings suggest that relying upon individual compliance significantly lowers the incidence of the disease, but does not eradicate it. [Marwa et al. \(2018\)](#), incorporated water treatment as a control strategy with the class of infected individuals divided into symptomatic and asymptomatic infected individuals. Parameter estimation was done using least square and Markov Chain Monte Carlo (MCMC) methods. Their results suggest that both least squares and MCMC methods performed well to the cholera model developed, and encouraged validation of the model using real data of cholera cases.

[Posny and Wang \(2014\)](#) proposed a deterministic compartmental model that incorporated seasonal variation into the general formulation of force of infection and pathogen concentration. To demonstrate this model, three specific examples of cholera models by [Codeço \(2001\)](#), [Mukandavire et al. \(2011\)](#) and [Tien and Earn \(2010\)](#) were used in the general analysis. Results were consistent with their analytical predictions. The conclusion was that seasonal variation significantly influences both environment-to-human and human-to-human routes disease dynamics. [Abdulrahim and Adesola \(2022\)](#) did a review on antimicrobial resistance (AMR) in cholera and concluded that Antimicrobials are not effective in cholera therapy. They suggested that vaccines, probiotics, phage therapy and improvements in hygiene practices, such as hand-washing and the accessibility of safe water, will significantly help to prevent cholera outbreaks.

[D'Mello-Guyett et al. \(2020\)](#), did a review of current WASH intervention protocols applied in cholera response programs in areas with ongoing transmission and during outbreaks. The recommended WASH interventions were extracted, categorised and analysed based on consistency and concordance. They were classified on the basis of whether they targeted within-household or community-level transmission. Results showed that most of the proposed measures focused on transmission at the community level while the remainder addressed within-household transmission or a combination of both. Proof from recent studies however suggest that for effective cholera control, interventions should concentrate on individualized approaches and transmission within the household. ([D'Mello-Guyett et al., 2020](#)).

A review by [Usmani et al. \(2021\)](#), described two components key to cholera outbreak; trigger and transmission components. They described trigger modules (TM) as processes that enable

reproduction, replication, survival, and distribution of *V. cholerae* in the environment whereas transmission component (TrM) as channels through which cholera spreads. The authors argued that the cholera spread is a complex result of global travel and the increased risk of populations being exposed to new disease outbreaks, influenced by both spatial and temporal factors, alongside climatic conditions (Usmani et al., 2021). A hypothesis proposed by Jutla et al. (2013), stated that unusually high temperatures, followed by equally high rainfall over a four-week period, in regions with weakened or damaged WASH infrastructure, created conditions that facilitated the interaction between contaminated water and human populations, thus creating an environment conducive to triggering a cholera epidemic. The theory was supported by spatial and temporal evidence from various regions, including South Sudan, Cameroon, and Zimbabwe. (Usmani et al., 2021). Subsequently, the theory was expanded to assess the impact of disasters on the likelihood of cholera outbreaks.

Wang et al. (2018), proposed a deterministic model that investigates the spatiotemporal dynamics of cholera transmission. Their model utilizes the reaction–convection–diffusion processes to represent the spatial movement of the hosts and pathogens, and the periodic contact and growth rates to describe the seasonality of the disease transmission, thereby integrating both the spatial and seasonal dynamics in one framework. The results of their analysis showed that host movement and pathogen dispersal elevate the risk of infection. The authors illustrated that reducing activity levels of infected persons and limiting their travels could weaken the host diffusion. Moreover, using water sanitation as an intervention could decrease pathogen dispersal (Wang et al., 2018).

Bakare and Hoskova-Mayerova (2021) developed deterministic and stochastic mathematical models of cholera transmission and control dynamics that were used to investigate the effect of three control interventions including the use of hygiene promotion and social mobilization; the use of treatment by drug/oral re-hydration solution; and the use of safe water, hygiene, and sanitation, against cholera transmission, in order to find optimal control strategies. The authors used the Pontryagin's maximum principle to characterize the optimal levels of combined control interventions. Optimal control theory revealed that the combinations of the control intervention influenced disease progression. Combinations of all three control

interventions was the optimal control strategy to effectively control cholera transmission, mortality, and morbidity.

A study by [Phan et al. \(2021\)](#), proposed a stochastic model for cholera epidemics that integrated environmental fluctuations with nonlinear system of Itô stochastic differential equations. The authors conducted an asymptotical analysis of dynamical behaviors for the model. They demonstrate existence of a unique stationary ergodic distribution to which all solutions of the stochastic model approaches when the noise intensities are bounded. When the basic reproduction number for the corresponding deterministic model is greater than 1, and the noise intensities are large enough such that the basic stochastic reproduction value is less than 1, the cholera infection is suppressed by environmental noises ([Phan et al., 2021](#)).

2.2.1 Research Gap

Beneficial outcomes have been produced with the help of these studies. However, the use of WASH as an intervention has been very minimal. The model proposed here incorporates WASH intervention to the existing Susceptible-Infected-Recovered-Vaccinated-Bacteria model. Moreover, it integrates the treatment compartment that accounts for those individuals who undergo formal medical treatment, and distinguishes them from individuals that survive infection with natural recovery. This is an extension of the model proposed by [Maliki and Chibuike \(2021\)](#), that incorporated WASH and treatment without natural recovery. In this work, the effect of enhanced sanitation facilities with vaccination and treatment on cholera transmission dynamics will be assessed. [Edward and Nyerere \(2015\)](#) showed that multiple control measures were effective as compared to a single control. Here, outcomes of different WASH interventions will be compared, and the most effective combinations of the strategies will be identified, also in consideration of a resource limited setting. The novelty in this work encompasses the incorporation of WASH, vaccination, treatment, direct and indirect transmission and model verification through sensitivity analysis, all in one single framework. The model will seek to determine the underlying aspects of cholera transmission dynamics and the effectiveness of probable interventions.

Chapter 3

Methodology

3.1 Model Formulation

To assess the effects of enhanced WASH in the presence of vaccination and treatment on cholera transmission, a deterministic disease model is used. The model consists of two populations; the human and the cholera bacteria population. The human population is divided into five compartments; individuals susceptible to the disease (S), individuals vaccinated (V), infected individuals who were not treated (I_n), treated individuals who were infected (T_i) and recovered individuals (R). The concentration of bacteria *Vibrio cholerae* in the environment is denoted by B . The susceptible population is recruited at a constant rate π through birth and a rate θ through waned immunity. They are vaccinated at a rate ν to progress to the vaccinated class V . We assume that vaccination confers complete protection against cholera infection, and therefore vaccinated individuals do not move to the infected compartments. The assumption simplifies the model and is supported by the high efficacy of some oral cholera vaccines. However, the assumption can be relaxed in future work to account for partial protection. Immunity is temporary and is lost at a rate θ . Populations in these compartments are reduced by natural death at the rate μ_1 .

Upon exposure to bacteria in the environment and contact with infected individuals, newly infected individuals progress to the untreated infected class I_n through the force of infection Λ . The force of infection is given by

$$\Lambda = \left(\frac{\beta_e(1 - \omega_1)B}{K + B} + \frac{(1 - \omega_2)}{N}(\beta_h I_n + \beta_{hT} T_i) \right) \quad (3.1)$$

where β_e is the rate of infection from *Vibrio cholerae*, and β_h and β_{hT} are the rates of infection from infected individuals I_n and T_i respectively. These transmission rates (β_e , β_h and β_{hT}) are controlled by ω_1 and ω_2 , which are the effectiveness of WASH in reducing transmission through the environment (for instance by use of water treatment, chlorination of water sources) and through direct human contact (by implementing hand hygiene, hygienic practices in food handling, proper sanitation infrastructure) respectively. The parameters are such that $0 \leq \omega_1, \omega_2 \leq 1$. K is the half saturation constant. It is the concentration of the pathogen that increases the likelihood of infection from consumption of pathogen from the environment to 50%.

Individuals in I_n may recover naturally at rate γ , or seek treatment at rate τ . We assume that disease induced death occurs at a rate μ_2 . Individuals diagnosed with cholera may progress to the treatment class T_i at rate τ where they either recuperate at a rate α and move to the recovered class R , or die naturally. The recovered class is replenished by individuals who recover naturally at the rate γ and those who recover due to treatment at the rate α , and reduced by natural death. Finally, the bacteria concentration in the environment is brought about by bacteria shedding from treated infected individuals at rate ε_T and untreated infected individuals at rate ε_u . These rates are controlled by ω_3 (the effectiveness of WASH in reducing bacterial shedding by implementing safe fecal sludge management, proper sanitation infrastructure, proper wastewater treatment). The bacteria population is depleted by natural death δ , enhanced by the rate ω_4 ($0 \leq \omega_4 \leq 1$), which denotes the effectiveness of WASH in increasing bacterial decay (by water treatment, disinfection and waste water treatment). The conceptual framework that described the above dynamics is as shown in Figure 3.1.

3.1.1 Compartmental Model

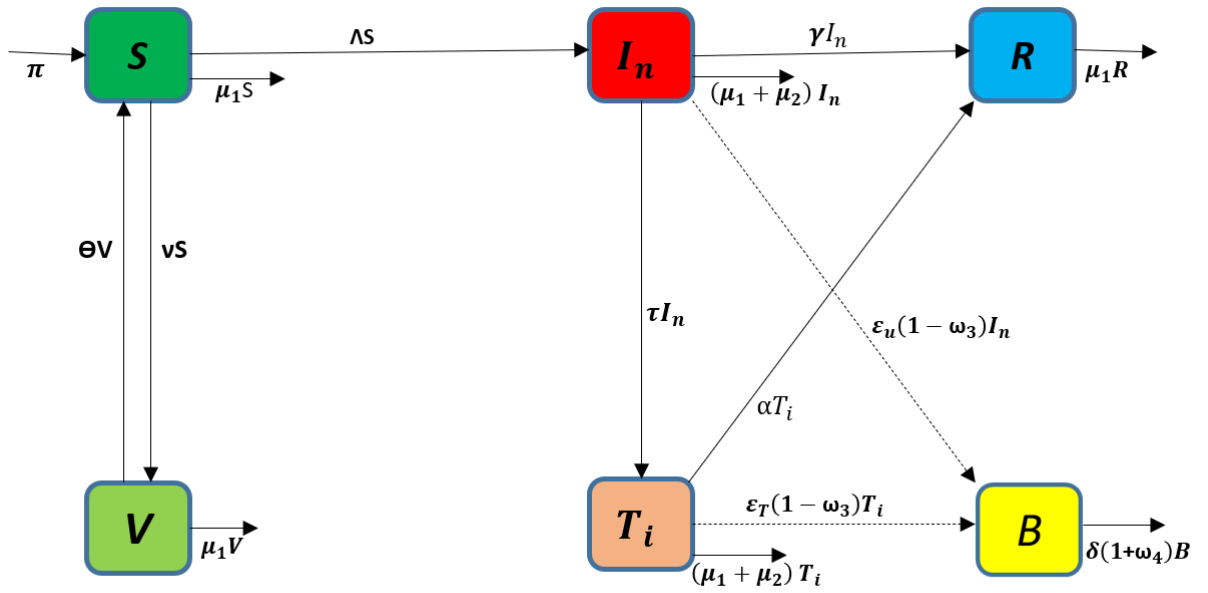


Figure 3.1: Cholera dynamics conceptual model. See Equation (3.1) for definition of Λ

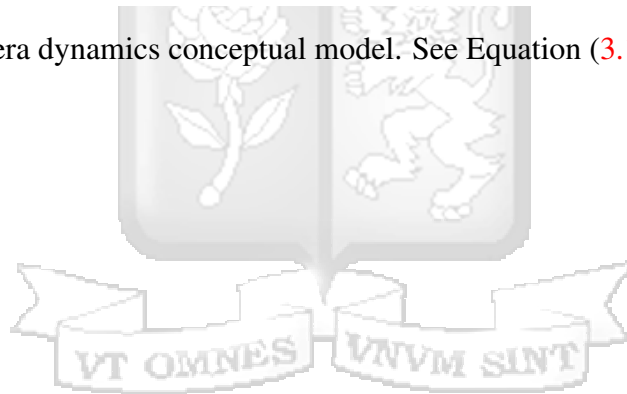


Table 3.1: Model parameters

Parameter	Description
β_e	Rate of infection from cholera contaminated environment
β_h	Rate of infection through human-to-human interaction from untreated infected individuals
β_{hT}	Rate of infection from treated infected individuals
K	Bacteria concentration at which the transmission rate is half its maximum value
ϵ_u	Bacteria shedding rate by a untreated infected individual
ϵ_T	Bacteria shedding rate by a treated infected individual
π	Human recruitment rate
μ_1	Human natural death rate
μ_2	Disease induced death rate on humans
δ	Rate of decay of cholera bacteria
γ	Natural recovery rate of untreated infected individuals
α	Recovery rate of treated infected individuals
ω_1	effectiveness of WASH in reducing transmission through the environment
ω_2	effectiveness of WASH in reducing transmission through direct human contact
ω_3	effectiveness of WASH in reducing bacterial shedding
ω_4	effectiveness of WASH in increasing bacterial decay
τ	Human treatment rate
ν	Human vaccination rate
θ	Rate of waning of immunity

3.1.2 Model Equations

The model system of equations that describes the cholera dynamics is given by

$$\begin{aligned}
 \frac{dS}{dt} &= \pi + \theta V - \Lambda S - (\mu_1 + \nu)S, \\
 \frac{dI_n}{dt} &= \Lambda S - (\mu_1 + \mu_2 + \gamma + \tau)I_n, \\
 \frac{dT_i}{dt} &= \tau I_n - (\mu_1 + \mu_2 + \alpha)T_i, \\
 \frac{dV}{dt} &= \nu S - (\theta + \mu_1)V, \\
 \frac{dR}{dt} &= \gamma I_n + \alpha T_i - \mu_1 R, \\
 \frac{dB}{dt} &= \varepsilon_T(1 - \omega_3)T_i + \varepsilon_u(1 - \omega_3)I_n - \delta(1 + \omega_4)B,
 \end{aligned} \tag{3.2}$$

where

$$\Lambda = \left(\frac{\beta_e(1 - \omega_1)B}{K + B} + \frac{(1 - \omega_2)}{N}(\beta_h I_n + \beta_{hT} T_i) \right),$$

with positive initial conditions given by

$$\begin{aligned}
 S(0) &> 0, & V(0) &\geq 0, & I_n(0) &\geq 0, \\
 T_i(0) &\geq 0, & R(0) &\geq 0, & B(0) &\geq 0.
 \end{aligned}$$

3.2 Model properties

In this section, we show that our model is well-posed mathematically and biologically, by investigating the positivity and boundedness of solutions.

3.2.1 Positivity of Solutions

Given that the model encompasses the human and bacteria population, we shall prove that all solutions of the system of equations, with positive initial conditions are positive for all $t \geq 0$.

Theorem 3.1. *For the given initial conditions, the solutions of model system (3.2) remains positive for all $t \geq 0$*

Proof. Consider the first equation in the system (3.2)

$$\frac{dS}{dt} = \pi + \theta V - \Lambda S - \mu_1 S - \nu S.$$

$$\frac{dS}{dt} = \pi + \theta V - (\Lambda + \mu_1 + \nu) S.$$

We have that

$$\frac{dS}{dt} \geq -(\Lambda + \mu_1 + \nu) S.$$

By separating the variables

$$\frac{dS}{S} \geq -(\Lambda + \mu_1 + \nu) dt.$$

Integrating

$$\int \frac{dS}{S} \geq - \int (\Lambda + \mu_1 + \nu) dt,$$

$$\ln S(t) - \ln S(0) = \ln \left(\frac{S(t)}{S(0)} \right) \geq - \left(\mu_1 t + \nu t + \int_0^t \Lambda(\zeta) d\zeta \right).$$

Taking the exponential of both sides:

$$\frac{S(t)}{S(0)} \geq e^{-(\mu_1 t + \nu t + \int_0^t \Lambda(\zeta) d\zeta)},$$

$$S(t) \geq S(0) e^{-(\mu_1 t + \nu t + \int_0^t \Lambda(\zeta) d\zeta)}. \quad (3.3)$$

Since the exponential function is positive and $S(0) > 0$, it is guaranteed that the solution of $S(t)$ remains positive for all time $t \geq 0$.

In a similar way, this procedure can be applied to all the remaining five equations of the system, so that we have the following solutions:

$$V(t) \geq V(0) e^{-(\theta + \mu_1)t}, \quad (3.4)$$

$$I_n(t) \geq I_n(0) e^{-(\mu_1 + \mu_2 + \gamma + \tau)t}, \quad (3.5)$$

$$T_i(t) \geq T_i(0) e^{-(\mu_1 + \mu_2 + \gamma t)t}, \quad (3.6)$$

$$R(t) \geq R(0) e^{-\mu_1 t}, \quad (3.7)$$

$$B(t) \geq B(0) e^{-\delta(1-\omega_4)t}. \quad (3.8)$$

Therefore, the solution of model system is always positive. \square

3.2.2 Boundedness of Solutions

We also need to show that the solutions are bounded for all $t \geq 0$ in the positive region Ω , where Ω is a biologically realistic region, and the model should be biologically meaningful.

$$\Omega = \left\{ \Omega_1 \times \Omega_2 \in \mathbb{R}_+^6 \right\},$$

where

$$\Omega_1 = \left\{ (S, V, I_n, T_i, R) \in \mathbb{R}_+^5 : 0 < S + V + I_n + T_i + R \leq \frac{\pi}{\mu_1} \right\},$$

$$\Omega_2 = \left\{ B \in \mathbb{R}_+^1 : 0 \leq B \leq \frac{\varepsilon_1 I_v + \varepsilon_2 I_n}{\mu_3 + \omega} \right\}.$$

Theorem 3.2. *The solutions of the model system (3.2) with the given initial conditions are contained in the region Ω .*

Proof. Consider the human population

$$N(t) = S(t) + V(t) + I_n(t) + T_i(t) + R(t).$$

We have;

$$\frac{dN(t)}{dt} = \frac{dS(t)}{dt} + \frac{dV(t)}{dt} + \frac{dI_n(t)}{dt} + \frac{dT_i(t)}{dt} + \frac{dR(t)}{dt},$$

or

$$\frac{dN(t)}{dt} = \pi - (S + V + I_n + T_i + R)\mu_1 - (I_n + T_i)\mu_2,$$

$$\frac{dN(t)}{dt} = \pi - N\mu_1 - I\mu_2,$$

which simplifies to

$$\frac{dN(t)}{dt} \leq \pi - N\mu_1,$$

or

$$\frac{dN(t)}{dt} + N\mu_1 \leq \pi. \quad (3.9)$$

Multiplying equation (3.9) all through by integrating factor, $e^{\mu_1 t}$, we get:

$$\frac{dN(t)}{dt} e^{\mu_1 t} + N\mu_1 e^{\mu_1 t} \leq \pi e^{\mu_1 t}.$$

By product rule, $d(N(t)e^{\mu_1 t}) \leq \pi e^{\mu_1 t} dt$.

Integrating yields:

$$\int d(N(t)e^{\mu_1 t}) \leq \int \pi e^{\mu_1 t} dt,$$

$$N(t)e^{\mu_1 t} \leq \frac{\pi}{\mu_1} e^{\mu_1 t} + A_1,$$

$$N(t) \leq \frac{\pi}{\mu_1} + A_1 e^{-\mu_1 t}.$$

(3.10)

As $t \rightarrow \infty$, $N(t) \leq \frac{\pi}{\mu_1}$.

If $N(0) < \frac{\pi}{\mu_1}$, then the upper bound of $N(t)$ is $\frac{\pi}{\mu_1}$ when $t \rightarrow \infty$. If $N(0) \geq \frac{\pi}{\mu_1}$, then $N(t)$ decreases to $\frac{\pi}{\mu_1}$ when $t \rightarrow \infty$ and approaches Ω asymptotically. Since N is the sum of the human state space variables, each of the individual state variables is less or equal to $\frac{\pi}{\mu_1}$.

Also, consider the bacteria population:

$$\frac{dB}{dt} = \varepsilon_T(1 - \omega_3)T_i + \varepsilon(1 - \omega_3)I_n - \delta(1 - \omega_4)B.$$

Since $I_n \leq \frac{\pi}{\mu_1}$ and $T_i \leq \frac{\pi}{\mu_1}$,

$$\begin{aligned}\frac{dB}{dt} &\leq \varepsilon_T(1-\omega_3)\frac{\pi}{\mu_1} + \varepsilon(1-\omega_3)\frac{\pi}{\mu_1} - \delta(1-\omega_4)B, \\ \frac{dB}{dt} + \delta(1-\omega_4)B &\leq \varepsilon_T(1-\omega_3)\frac{\pi}{\mu_1} + \varepsilon(1-\omega_3)\frac{\pi}{\mu_1}.\end{aligned}\quad (3.11)$$

Multiplying equation (3.11) all through by integrating factor, $e^{\delta(1-\omega_4)t}$, gives:

$$\frac{dB}{dt}e^{\delta(1-\omega_4)t} + \delta(1-\omega_4)Be^{\delta(1-\omega_4)t} \leq \varepsilon_T(1-\omega_3)\frac{\pi}{\mu_1}e^{(\mu_3+\omega)t} + \varepsilon(1-\omega_3)\frac{\pi}{\mu_1}e^{\delta(1-\omega_4)t}.$$

By product rule,

$$d(Be^{\delta(1-\omega_4)t}) \leq \left(\varepsilon_T(1-\omega_3)\frac{\pi}{\mu_1} + \varepsilon(1-\omega_3)\frac{\pi}{\mu_1} \right) e^{\delta(1-\omega_4)t} dt.$$

Integrating gives:

$$Be^{\delta(1-\omega_4)t} \leq \frac{\left(\varepsilon_T(1-\omega_3)\frac{\pi}{\mu_1} + \varepsilon(1-\omega_3)\frac{\pi}{\mu_1} \right) e^{\delta(1-\omega_4)t}}{\delta(1-\omega_4)} + A_2,$$

$$B \leq \frac{\left(\varepsilon_T(1-\omega_3)\frac{\pi}{\mu_1} + \varepsilon(1-\omega_3)\frac{\pi}{\mu_1} \right)}{\delta(1-\omega_4)} + A_2 e^{-\delta(1-\omega_4)t}.$$

$$\text{As } t \rightarrow \infty, B(t) \leq \frac{\left(\varepsilon_T(1-\omega_3)\frac{\pi}{\mu_1} + \varepsilon(1-\omega_3)\frac{\pi}{\mu_1} \right)}{\delta(1-\omega_4)} \quad \text{or} \quad B(t) \leq \frac{\varepsilon_T(1-\omega_3) + \varepsilon(1-\omega_3)\pi}{\delta(1-\omega_4)\mu_1}.$$

Hence, we have that $0 \leq N(t) \leq \frac{\pi}{\mu_1}$ and $0 \leq B(t) \leq \frac{\varepsilon_T(1-\omega_3) + \varepsilon(1-\omega_3)\pi}{\delta(1-\omega_4)\mu_1}$ which implies that B, N and each of the individual state variables S, V, I_u, T_i, R are bounded and all solutions starting in Ω stay in Ω . \square

3.3 Equilibria Points and Stability Analysis

3.3.1 Disease Free Equilibrium Point

This is the point at which no disease is present in the population. Our model always has a disease free equilibrium (DFE). In the absence of infection, $I_u = T_i = B = 0$. This implies that our DFE, E_0 , is

$$E^0 = (S, V, I_n, T_i, R, B) = \left(\frac{\pi(\theta + \mu_1)}{\mu_1(\theta + \mu_1 + \nu)}, \frac{\pi\nu}{\mu_1(\theta + \mu_1 + \nu)}, 0, 0, 0, 0 \right). \quad (3.12)$$

3.3.2 Effective Reproduction Number

The effective reproduction number R_v is the number of secondary cases produced by one infected individual in a population that is not completely susceptible. Using the next-generation operator method by van den Driessche and Watmough ([Van den Driessche and Watmough, 2002](#)), the system of ordinary differential equations of the infectious compartments $X(i)$ can be written as

$$\frac{dX_i}{dt} = F_i - V_i,$$

where F_i represents the rate at which new infections appear in compartment i and V_i represents the rate at which individuals transfer from compartment i . R_v is then obtained by taking the largest/dominant eigenvalue of

$$\left[\frac{\delta F_i(E_0)}{\delta X_i} \right] \left[\frac{\delta V_i(E_0)}{\delta X_i} \right]^{-1},$$

where E_0 is the disease free equilibrium.

We therefore have $\frac{dX(i)}{dt}$ as

$$\begin{aligned}\frac{dI_n}{dt} &= \left(\frac{\beta_e(1-\omega_1)B}{K+B} + \frac{\beta_h(1-\omega_2)I_n}{N} + \frac{\beta_{hT}(1-\omega_2)T_i}{N} \right) S - (\mu_1 + \mu_2 + \gamma + \tau)I_n, \\ \frac{dT_i}{dt} &= \tau I_u - (\mu_1 + \mu_2 + \alpha)T_i, \\ \frac{dB}{dt} &= \varepsilon_T(1-\omega_3)T_i + \varepsilon_u(1-\omega_3)I_n - \delta(1+\omega_4)B,\end{aligned}$$

and

$$F_i = \begin{pmatrix} \left(\frac{\beta_e(1-\omega_1)B}{K+B} + \frac{\beta_h(1-\omega_2)I_n}{N} + \frac{\beta_{hT}(1-\omega_2)T_i}{N} \right) S \\ 0 \\ 0 \end{pmatrix},$$

$$V_i = \begin{pmatrix} (\mu_1 + \mu_2 + \gamma + \tau)I_n \\ -\tau I_n + (\mu_1 + \mu_2 + \gamma_T)T_i \\ -\varepsilon_T(1-\omega_3)T_i - \varepsilon_u(1-\omega_3)I_n + \delta(1+\omega_4)B \end{pmatrix}.$$

The Jacobian of the above matrices is obtained as

$$F_i = \begin{pmatrix} \frac{\beta_h(1-\omega_2)S}{N} & \frac{\beta_{hT}(1-\omega_2)S}{N} & \frac{\beta_e(1-\omega_1)SK}{(K+B)^2} \\ 0 & 0 & 0 \\ 0 & 0 & 0 \end{pmatrix},$$

$$V_i = \begin{pmatrix} \mu_1 + \mu_2 + \gamma + \tau & 0 & 0 \\ -\tau & \mu_1 + \mu_2 + \gamma_T & 0 \\ -\varepsilon_u(1-\omega_3) & -\varepsilon_T(1-\omega_3) & \delta(1+\omega_4) \end{pmatrix}.$$

At E_0 , we have;

$$\mathcal{F} = \begin{pmatrix} \frac{\beta_h(1-\omega_2)(\theta + \mu_1)}{\theta + \mu_1 + \nu} & \frac{\beta_{hT}(1-\omega_2)(\theta + \mu_1)}{\theta + \mu_1 + \nu} & \frac{\beta_e(1-\omega_1)\pi(\theta + \mu_1)}{K\mu_1(\theta + \mu_1 + \nu)} \\ 0 & 0 & 0 \\ 0 & 0 & 0 \end{pmatrix},$$

$$\mathcal{V} = \begin{pmatrix} \mu_1 + \mu_2 + \gamma + \tau & 0 & 0 \\ -\tau & \mu_1 + \mu_2 + \alpha & 0 \\ -\varepsilon_u(1-\omega_3) & -\varepsilon_T(1-\omega_3) & \delta(1+\omega_4) \end{pmatrix}.$$

The inverse of matrix \mathcal{V} is given as

$$\mathcal{V}^{-1} = \begin{pmatrix} \frac{1}{\mu_1 + \mu_2 + \gamma + \tau} & 0 & 0 \\ \frac{(\alpha + \mu_1)(\gamma + \tau + \mu_1 + \mu_2)}{\tau} & \frac{1}{\mu_1 + \mu_2 + \gamma_T} & 0 \\ \frac{\varepsilon_u \alpha + \tau \varepsilon_T + \varepsilon_u \mu_1 - \varepsilon_u \alpha \omega_3 - \tau \varepsilon_T \omega_3 - \varepsilon_u \mu_1 \omega_3}{\delta(\alpha + \mu_1 + \mu_2)(\gamma + \tau + \mu_1 + \mu_2)(1 + \omega_4)} & \frac{\varepsilon_T(1 - \omega_3)}{\delta(\alpha + \mu_1 + \mu_2)(1 + \omega_4)} & \frac{1}{\delta(1 + \omega_4)} \end{pmatrix}.$$

Multiplying \mathcal{F} with \mathcal{V}^{-1} , we get

$$\begin{pmatrix} A & B & C \\ 0 & 0 & 0 \\ 0 & 0 & 0 \end{pmatrix},$$

where

$$\begin{aligned} A &= \frac{(1 - \omega_2) \beta_h (\theta + \mu_1)}{(\gamma + \mu_1 + \mu_2 + \tau) (\theta + \mu_1 + \nu)} \\ &+ \frac{(1 - \omega_2) (\theta + \mu_1) \beta_{hT} (\delta \tau \omega_4 + \delta \tau)}{\delta (\omega_4 + 1) (\gamma + \mu_1 + \mu_2 + \tau) (\theta + \mu_1 + \nu) (\mu_1 + \mu_2 + \alpha)} \\ &+ \frac{\beta_e \pi (1 - \omega_1) (\theta + \mu_1) (\varepsilon_u (1 - \omega_3) (\mu_1 + \mu_2 + \alpha) + \tau (1 - \omega_3) \varepsilon_T)}{\delta K \mu_1 (\omega_4 + 1) (\gamma + \mu_1 + \mu_2 + \tau) (\theta + \mu_1 + \nu) (\mu_1 + \mu_2 + \alpha)}, \\ B &= \frac{(1 - \omega_2) (\theta + \mu_1) \beta_{hT}}{(\theta + \mu_1 + \nu) (\mu_1 + \mu_2 + \alpha)} + \frac{\beta_e \pi (1 - \omega_1) (1 - \omega_3) (\theta + \mu_1) \varepsilon_T}{\delta K \mu_1 (\omega_4 + 1) (\theta + \mu_1 + \nu) (\mu_1 + \mu_2 + \alpha)}, \\ C &= \frac{\beta_e \pi (1 - \omega_1) (\theta + \mu_1)}{\delta K \mu_1 (\omega_4 + 1) (\theta + \mu_1 + \nu)}. \end{aligned}$$

The spectral radius of matrix (3.3.2), is the dominant eigenvalue described as;

$$R_v = R_h + R_e, \quad (3.13)$$

where

$$R_h = \frac{\beta_h(\theta + \mu_1)(1 - \omega_2)}{(\theta + \nu + \mu_1)(\gamma + \tau + \mu_1 + \mu_2)} + \frac{\tau\beta_{hT}(1 - \omega_2)(\theta + \mu_1)}{(\alpha + \mu_1 + \mu_2)(\theta + \nu + \mu_1)(\gamma + \tau + \mu_1 + \mu_2)},$$

$$R_e = \frac{\beta_e\pi(\theta + \mu_1)(1 - \omega_1)[\tau\varepsilon_T(1 - \omega_3) + \varepsilon(1 - \omega_3)(\gamma_T + \mu_1 + \mu_2)]}{K\mu_1\delta(\alpha + \mu_1 + \mu_2)(\gamma + \tau + \mu_1 + \mu_2)(1 + \omega_4)(\theta + \nu + \mu_1)}.$$

The progression of the disease depends on the reproduction number of an infected individual and bacteria in the environment. If $R_h > R_e$, the infection is propelled by human-to-human interaction. In this case, sanitation practices that limit contact with infected individuals should be observed in order to manage the infection. In contrast, if $R_e > R_h$, the infection is mainly propagated by contact of individuals with bacteria in the environment. In this conditions, WASH interventions increasing the rate of bacteria decay, reducing bacteria ingestion and shedding should be implemented.

Observe that $R_h = R_{hi} + R_{hT}$. Here, R_{hi} is the reproduction number due interaction of susceptible individuals with infected individuals who are not under treatment and R_{hT} is the reproduction number due interaction of susceptible individuals with infected individuals who receive treatment.

3.3.3 Local Stability of Disease Free Equilibrium

The local stability analysis of the disease- free equilibrium point (DFE) of the model is determined by finding the Jacobian matrix and its eigenvalues. An equilibrium point is locally asymptotically stable if all the eigenvalues of the jacobian matrix at that point are negative. Local stability of the DFE can be analyzed using the reproduction number R_v . The DFE is locally asymptotically stable if $R_v < 1$ and unstable when $R_v > 1$. The general Jacobian matrix of model is written as:

$$\begin{pmatrix} -(a+\mu_1+\nu) & -\frac{\beta_h(1-\omega_2)S}{N} & -\frac{\beta_{hT}(1-\omega_2)S}{N} & \theta & 0 & 0 \\ a & \frac{\beta_h(1-\omega_2)S}{N} - (\mu_1+\mu_2+\gamma+\tau) & \frac{\beta_{hT}(1-\omega_2)S}{N} & 0 & 0 & 0 \\ 0 & \tau & -(\mu_1+\alpha) & 0 & 0 & 0 \\ \nu & 0 & 0 & -(\theta+\mu_1) & 0 & 0 \\ 0 & \gamma & \alpha & 0 & -\mu_1 & 0 \\ 0 & \varepsilon_u(1-\omega_3) & \varepsilon_T(1-\omega_3) & 0 & 0 & -\delta(1+\omega_4) \end{pmatrix}, \quad (3.14)$$

where $a = \frac{\beta_e(1-\omega_1)B}{K+B} + \frac{\beta_h(1-\omega_2)I_n}{N} + \frac{\beta_{hT}(1-\omega_2)T_i}{N}$.

The jacobian at the disease free equilibrium is given as

$$\begin{pmatrix} -(\mu_1+\nu) & \frac{-\beta_h(1-\omega_2)(\theta+\mu_1)}{(\theta+\mu_1+\nu)} & \frac{-\beta_{hT}(1-\omega_2)(\theta+\mu_1)}{(\theta+\mu_1+\nu)} & \theta & 0 & 0 \\ 0 & \frac{\beta_h(1-\omega_2)(\theta+\mu_1)}{(\theta+\mu_1+\nu)} - (\mu_1+\mu_2+\gamma+\tau) & \frac{\beta_{hT}(1-\omega_2)(\theta+\mu_1)}{(\theta+\mu_1+\nu)} & 0 & 0 & 0 \\ 0 & \tau & -(\mu_1+\alpha) & 0 & 0 & 0 \\ \nu & 0 & 0 & -(\theta+\mu_1) & 0 & 0 \\ 0 & \gamma & \alpha & 0 & -\mu_1 & 0 \\ [6pt] 0 & \varepsilon_u(1-\omega_3) & \varepsilon_T(1-\omega_3) & 0 & 0 & -\delta(1+\omega_4) \end{pmatrix}. \quad (3.15)$$

From the fourth, fifth and sixth columns in the matrix above, it is clear that $-(\theta+\mu_1)$, $-\mu_1$ and $-\delta(1-\omega_4)$ are the first three eigenvalues. Upon deletion of the fourth, fifth and sixth columns and rows, we have our matrix reduced as;

$$\begin{pmatrix} -(\mu_1+\nu) & \frac{-\beta_h(1-\omega_2)(\theta+\mu_1)}{(\theta+\mu_1+\nu)} & \frac{-\beta_{hT}(1-\omega_2)(\theta+\mu_1)}{(\theta+\mu_1+\nu)} \\ 0 & \frac{\beta_h(1-\omega_2)(\theta+\mu_1)}{(\theta+\mu_1+\nu)} - (\mu_1+\mu_2+\gamma+\tau) & \frac{\beta_{hT}(1-\omega_2)(\theta+\mu_1)}{(\theta+\mu_1+\nu)} \\ 0 & \tau & -(\mu_1+\alpha) \end{pmatrix}. \quad (3.16)$$

From matrix (3.16), we can clearly see that the fourth eigenvalue is $-(\mu_1 + \nu)$ from the first column. Upon removal of the first row and column, we have the following reduced matrix.

$$\begin{pmatrix} \frac{\beta_h(1-\omega_2)(\theta + \mu_1)}{(\theta + \mu_1 + \nu)} - (\mu_1 + \mu_2 + \gamma + \tau) & \frac{\beta_{hT}(1-\omega_2)(\theta + \mu_1)}{(\theta + \mu_1 + \nu)} \\ \tau & -(\mu_1 + \alpha) \end{pmatrix}. \quad (3.17)$$

The remaining two eigenvalues can be obtained by finding the roots of the following characteristic polynomial associated with matrix (3.17)

$$P(\lambda) = \lambda^2 + P_1\lambda + P_2, \quad (3.18)$$

where

$$P_1 = \gamma + \tau + \alpha + \mu_1 + \mu_2 - \frac{\beta_h(\theta + \mu_1)(1 - \omega_2)}{\theta + \mu_1 + \nu}$$

and

$$P_2 = \frac{(\alpha + \mu_1)[(\theta + \mu_1 + \nu)(\gamma + \tau + \mu_1 + \mu_2) + \beta_h(\theta + \mu_1)(\omega_2 - 1)] + \tau\beta_{hT}(\theta + \mu_1)(\omega_2 - 1)}{\theta + \nu + \mu_1}.$$

Based on the Routh–Hurwitz criterion, if $P_1 > 0$ and $P_1P_2 > 0$ then E_0 will be locally asymptotically stable when $R_v < 1$.

3.3.4 Global Stability of Disease Free Equilibrium

Here, we show that the cholera-free-equilibrium state is globally asymptotically stable when $R_v < 1$. Writing the model system in the pseudotriangular form, we have

$$\begin{aligned} \dot{X}_1 &= A_1(X_1 - X_1^*) + A_2X_2, \\ \dot{X}_2 &= A_3X_2, \end{aligned}$$

where X_1 is a vector denoting the number of uninfected states and X_2 is a vector denoting infected states.

$$X_1 = (S, V, R), \quad (3.19)$$

$$X_2 = (I_n, T_i, B).$$

From X_1 ,

$$A_1 = \begin{pmatrix} -(\mu_1 + \nu) & \theta & 0 \\ \nu & -(\theta + \mu_1) & 0 \\ 0 & 0 & -\mu_1 \end{pmatrix},$$

$$A_2 = \begin{pmatrix} -\beta_h(1 - \omega_2) & -\beta_{hT}(1 - \omega_2) & -\frac{\beta_e \pi(1 - \omega_1)(\theta + \mu_1)}{K\mu_1(\theta + \mu_1 + \nu)} \\ 0 & 0 & 0 \\ \gamma & \alpha & 0 \end{pmatrix}.$$

It can be observed that matrix A_1 has real and negative eigenvalues. This shows that the subsystem $\dot{X}_1 = A_1(X_1 - X_1^*) + A_2X_2$ is globally asymptotically stable at the disease free equilibrium E_0 . Similarly, from the subsystem X_2 we obtain the following matrix;

$$A_3 = \begin{pmatrix} -((\mu_1 + \mu_2 + \gamma + \tau) - \beta_h(1 - \omega_2)) & \beta_{hT}(1 - \omega_2) & \frac{\beta_e \pi(1 - \omega_1)(\theta + \mu_1)}{\mu_1(\theta + \mu_1 + \nu)} \\ \tau & -(\mu_1 + \alpha) & 0 \\ \varepsilon(1 - \omega_3) & \varepsilon_T(1 - \omega_3) & -\delta(1 + \omega_4) \end{pmatrix}. \quad (3.20)$$

In matrix 3.23, we note that the off-diagonal elements are positive, hence A_3 is a metzler matrix. To establish the global stability of the DFE, we need to show that matrix A_3 is Metzler stable. We apply the lemma used by Dumont et al. (2008) where A_3 is a Metzler matrix.

Lemma 3.1. *Let M be a square Metzler matrix written in block form $M = \begin{pmatrix} A & B \\ C & D \end{pmatrix}$ with A and D square matrices. M is Metzler stable if and only if matrices A and $D - CA^{-1}B$ are Metzler stable.*

In our case, we write the Metzler matrix A_3 as a square Metzler matrix

$$A_3 = \begin{pmatrix} A & B \\ C & D \end{pmatrix}, \quad (3.21)$$

such that the matrices A, B, C and D are defined as

$$A_{1 \times 1} = \left(-((\mu_1 + \mu_2 + \gamma + \tau) - \beta_h(1 - \omega_2)) \right) \quad B_{1 \times 2} = \left(\beta_{hT}(1 - \omega_2) \quad \frac{\beta_e \pi(1 - \omega_1)(\theta + \mu_1)}{\mu_1(\theta + \mu_1 + \nu)} \right)$$

$$C_{2 \times 1} = \left(\begin{array}{c} \tau \\ \varepsilon(1 - \omega_3) \end{array} \right) \quad D_{2 \times 2} = \left(\begin{array}{cc} -(\mu_1 + \gamma_T) & 0 \\ \varepsilon_T(1 - \omega_3) & -\delta(1 + \omega_4) \end{array} \right).$$

It is clear that A has a negative real eigenvalue making it a stable Metzler matrix. Based on mathematica software, matrix $D - CA^{-1}B$ is given as ;

$$\left(\begin{array}{cc} -\gamma_T - \mu_1 - \frac{\tau \beta_{hT}(1 - \omega_2)}{\beta_h(1 - \omega_2) - (\gamma + \tau + \mu_1 + \mu_2)} & -\frac{\pi \beta_e \tau(1 - \omega_1)(\theta + \mu_1)}{K \mu_1(\theta + \mu_1 + \nu)(\beta_h(1 - \omega_2) - \gamma - \mu_1 - \mu_2 - \tau)} \\ \varepsilon_T(1 - \omega_3) - \frac{\varepsilon \beta_{hT}(1 - \omega_2)(1 - \omega_3)}{\beta_h(1 - \omega_2) - (\gamma + \tau + \mu_1 + \mu_2)} & -\frac{\pi \beta_e \varepsilon(1 - \omega_1)(1 - \omega_3)(\theta + \mu_1)}{K \mu_1(\theta + \mu_1 + \nu)(\beta_h(1 - \omega_2) - \gamma - \mu_1 - \mu_2 - \tau)} - \delta(1 + \omega_4) \end{array} \right), \quad (3.22)$$

which can be written as;

$$\left(\begin{array}{cc} -\gamma_T - \mu_1 - \frac{\tau \beta_{hT}(1 - \omega_2)}{\beta_h(1 - \omega_2) - (\gamma + \tau + \mu_1 + \mu_2)} & -\frac{\pi \beta_e \tau(1 - \omega_1)(\theta + \mu_1)}{K \mu_1(\theta + \mu_1 + \nu)(\beta_h(1 - \omega_2) - \gamma - \mu_1 - \mu_2 - \tau)} \\ \varepsilon_T(1 - \omega_3) - \frac{\varepsilon \beta_{hT}(1 - \omega_2)(1 - \omega_3)}{\beta_h(1 - \omega_2) - (\gamma + \tau + \mu_1 + \mu_2)} & -\frac{\pi \beta_e \varepsilon(1 - \omega_1)(1 - \omega_3)(\theta + \mu_1)}{K \mu_1(\theta + \mu_1 + \nu)(\beta_h(1 - \omega_2) - (\gamma + \tau + \mu_1 + \mu_2))} - \delta(1 + \omega_4) \end{array} \right). \quad (3.23)$$

From matrix (3.23), all the diagonal elements are negative. This shows that the matrix $D - CA^{-1}B$ is metzler stable and the disease free equilibrium is globally asymptotically stable. All solutions starting in the feasible region of the model system (3.2) will converge to the DFE and cholera will be eradicated overtime in the presence of control interventions provided that $R_v < 1$.

3.4 Sensitivity Analysis

To evaluate the robustness of the model and determine the key parameters that influence cholera transmission dynamics, sensitivity analysis is performed. Using the normalised forward-sensitivity index, the relative change of R_v in response the relative change in a parameter is quantified. The normalised forward-sensitivity index of a variable, u , which

depends differentially on a parameter, ρ , is defined as;

$$\frac{\delta u}{\delta \rho} \times \frac{\rho}{u} . \quad (3.24)$$

Using the parameter values in Table 3.2 and mathematica software, the sensitivity for all the parameters in R_0 are calculated and presented in Table 3.3. A large numeric value of the sensitivity index implies a greater impact of the parameter on the disease progression. If the sensitivity index is positive, then the increasing the parameter value increases the basic reproduction number. However, if the sensitivity index is negative, then increasing the parameter value decreases the reproduction number.



Table 3.2: Parameter values

Symbol	Value	Source
β_e	0.214/day	Cui et al. (2014)
β_h	0.02	Cui et al. (2014)
β_{hT}	0.015	Assumed
K	10^6 cells/ml	Codeço (2001)
ϵ_u	10 cells/day	Kobe et al. (2018)
ϵ_T	5	Assumed
π	1500/day	Assumed
μ_1	0.0000431/day	Kobe et al. (2018)
μ_2	0.013/day	Cui et al. (2014)
δ	0.033/day	Onuorah et al. (2022)
γ	0.035/day	Njagarah and Nyabadza (2014)
α	0.0005	Assumed
ω_1	0.94	Assumed
ω_2	0.1095	Assumed
ω_3	0.94	Assumed
ω_4	0.73	Assumed
θ	0.025	Assumed
ν	0.04	Assumed
τ	0.3	Assumed

Table 3.3: Sensitivity indices (SI)

Parameter	SI	Parameter	SI
β_e	0.994499	τ	0.0553704
β_h	0.000312309	ω_1	-15.5805
β_{hT}	0.00518858	ω_2	-0.000676415
K	0.994499	ω_3	-15.5805
ε_u	0.0821551	ω_4	-0.419644
ε_T	0.912144	γ	-0.100562
π	0.994499	α	-0.0338672
μ_1	-0.997305	μ_2	-0.917898
θ	0.137489	ν	-0.137726
δ	-0.994499		

From the above results, β_e , K , ε_T , π , μ_1 , δ , ω_1 , ω_3 , and μ_2 are the most important parameters in cholera dynamics and control. The indices demonstrate that key targets for intervention are reducing transmission via the environment and shedding of bacteria. The results also show that the control measures that would have a greater impact on the cholera dynamics are the WASH interventions that reduce bacterial shedding into the environment (ω_3) and those that reduce transmission through the environment (ω_1). The rate of decay of bacteria has a significant effect on R_v and should be a priority area for intervention.

3.5 Optimal Control Analysis of WASH Interventions

The optimal time dependent controls ω_1 , ω_2 , ω_3 and ω_4 required to minimize the number of infective individuals I_n and T_i , and the density of bacteria B while accounting for the cost of implementing the WASH interventions, are determined. This is executed by minimizing the

following objective function.

$$J(\omega_1, \omega_2, \omega_3, \omega_4) = \int_0^T \left[C_1 I_n(t) + C_2 T_i(t) + C_3 B(t) + \frac{C_4}{2} \omega_1^2 + \frac{C_5}{2} \omega_2^2 + \frac{C_6}{2} \omega_3^2 + \frac{C_7}{2} \omega_4^2 \right] dt, \quad (3.25)$$

where $C_1, C_2, C_3, C_4, C_5, C_6$ and C_7 are positive weights and T is the final time.

The optimal control system is given by:

$$\begin{aligned} \frac{dS}{dt} &= \pi + \theta V - \left(\frac{\beta_e(1-\omega_1)B}{K+B} + \frac{\beta_h(1-\omega_2)I_n}{N} + \frac{\beta_{hT}(1-\omega_2)T_i}{N} \right) S - (\mu_1 + \nu)S, \\ \frac{dI_n}{dt} &= \left(\frac{\beta_e(1-\omega_1)B}{K+B} + \frac{\beta_h(1-\omega_2)I_n}{N} + \frac{\beta_{hT}(1-\omega_2)T_i}{N} \right) S - (\mu_1 + \mu_2 + \gamma + \tau)I_n, \\ \frac{dT_i}{dt} &= \tau I_n - (\mu_1 + \mu_2 + \alpha)T_i, \\ \frac{dV}{dt} &= \nu S - (\theta + \mu_1)V, \\ \frac{dR}{dt} &= \gamma I_n + \alpha T_i - \mu_1 R, \\ \frac{dB}{dt} &= \varepsilon_T(1-\omega_3)T_i + \varepsilon_u(1-\omega_3)I_n - \delta(1+\omega_4)B. \end{aligned} \quad (3.26)$$

with initial conditions

$$S(0) > 0, \quad V(0) \geq 0, \quad I_n(0) \geq 0,$$

$$T_i(0) \geq 0, \quad R(0) \geq 0, \quad B(0) \geq 0.$$

The goal is to seek an optimal control such that:

$$J(\omega_1^*, \omega_2^*, \omega_3^*, \omega_4^*) = \min\{J(\omega_1, \omega_2, \omega_3, \omega_4) | \omega_1, \omega_2, \omega_3, \omega_4 \in W\}, \quad (3.27)$$

where $W = (\omega_1, \omega_2, \omega_3, \omega_4)$ such that $\omega_1, \omega_2, \omega_3, \omega_4$ are measurable with $0 \leq \omega_1 \leq 1, 0 \leq \omega_2 \leq 1, 0 \leq \omega_3 \leq 1$ and $0 \leq \omega_4 \leq 1$ for $t \in [0, T]$ is the control set. We transform the problem into a Hamiltonian framework by introducing adjoint variables (λ) using Pontryagin's Maximum Principle. The Hamiltonian is given by:

$$H = C_1 I_n(t) + C_2(t) T_i + C_3 B(t) + \frac{C_4}{2} \omega_1^2 + \frac{C_5}{2} \omega_2^2 + \frac{C_6}{2} \omega_3^2 + \frac{C_7}{2} \omega_4^2 + \sum \lambda_i \frac{dX_i}{dt}, \quad (3.28)$$

where X_i are the state variables S, I_n, T_i, V, R, B , and λ_i are the adjoint variables.

Theorem 3.3. Suppose the set $\omega_1, \omega_2, \omega_3, \omega_4$ minimizes J over W , then the adjoint variables, $\lambda_S, \lambda_{I_n}, \lambda_{T_i}, \lambda_V, \lambda_R, \lambda_B$ satisfy the adjoint equations

$$-\frac{d\lambda}{dt} = \frac{dH}{dX}$$

with $\lambda(T) = 0$.

Proof. Consider $W = (\omega_1, \omega_2, \omega_3, \omega_4)$ and $S^*, I_n^*, T_i^*, V^*, R^*, B^*$ being the associated solutions. Pontryagin's maximum principle is applied, such that there exist adjoint variables satisfying:

$$\begin{aligned} -\frac{d\lambda_S}{dt} = \frac{dH}{dS} \quad \lambda_S(T) = 0, \quad -\frac{d\lambda_{I_n}}{dt} = \frac{dH}{dI_n} \quad \lambda_{I_n}(T) = 0, \\ -\frac{d\lambda_{T_i}}{dt} = \frac{dH}{dT_i} \quad \lambda_{T_i}(T) = 0, \quad -\frac{d\lambda_V}{dt} = \frac{dH}{dV} \quad \lambda_V(T) = 0, \\ -\frac{d\lambda_R}{dt} = \frac{dH}{dR} \quad \lambda_R(T) = 0, \quad -\frac{d\lambda_B}{dt} = \frac{dH}{dB} \quad \lambda_B(T) = 0, \end{aligned}$$

with $\lambda_S = \lambda_{I_n} = \lambda_{T_i} = \lambda_V = \lambda_R = \lambda_B = 0$. □

By the optimality conditions, we have

$$\begin{aligned} \frac{dH}{d\omega_1} &= C_4\omega_1 + \lambda_S\left(\frac{\beta_e BS}{K+B}\right) - \lambda_{I_n}\frac{\beta_e BS}{K+B} = 0, \\ \frac{dH}{d\omega_2} &= C_5\omega_2 + \lambda_S\left(\frac{\beta_h I_n S}{N} + \frac{\beta_{hT} T_i S}{N}\right) - \lambda_{I_n}\left(\frac{\beta_h I_n S}{N} + \frac{\beta_{hT} T_i S}{N}\right) = 0, \\ \frac{dH}{d\omega_3} &= C_6\omega_3 - \lambda_B(\varepsilon_T T_i + \varepsilon_u I_n) = 0, \\ \frac{dH}{d\omega_4} &= C_7\omega_4 + \lambda_B(\delta B) = 0. \end{aligned} \tag{3.29}$$

We have the optimal controls as:

$$\begin{aligned} \omega_1^* &= (\lambda_{I_n} - \lambda_S)\frac{\beta_e BS}{C_4(K+B)}, \\ \omega_2^* &= (\lambda_{I_n} - \lambda_S)\frac{(\beta_h I_n + \beta_{hT} T_i)S}{C_5 N}, \end{aligned}$$

$$\omega_3^* = \lambda_B \frac{\varepsilon_T T_i + \varepsilon_u I_n}{C_6},$$

$$\omega_4^* = -\lambda_B \frac{\delta B}{C_7}.$$

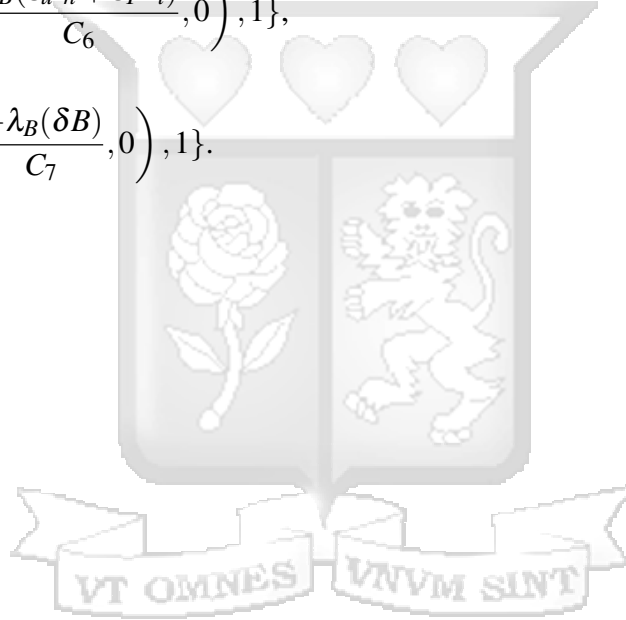
On the interior of the set, where $0 < \omega_j < 1$ for all $(j = 1, 2, 3, 4)$,

$$\omega_1^* = \min\left\{\max\left(\frac{(\lambda_{I_n} - \lambda_S)\beta_e B S}{C_4(K+B)}, 0\right), 1\right\},$$

$$\omega_2^* = \min\left\{\max\left(\frac{(\lambda_{I_n} - \lambda_S)(\beta_h I_n + \beta_{hT} T_i) S}{C_5 N}, 0\right), 1\right\},$$

$$\omega_3^* = \min\left\{\max\left(\frac{\lambda_B(\varepsilon_u I_n + \varepsilon_T T_i)}{C_6}, 0\right), 1\right\},$$

$$\omega_4^* = \min\left\{\max\left(\frac{-\lambda_B(\delta B)}{C_7}, 0\right), 1\right\}.$$



Chapter 4

Results and Discussion

4.1 Scenario Analysis of the Impact of Control Strategies

Numerical simulations of the cholera model (3.2) were conducted using the fourth-order Runge-Kutta method implemented in R. This method was chosen because it offers a balance between accuracy and computational efficiency, particularly for non-stiff problems that are mainly encountered in compartmental modeling. The initial conditions of state variables are chosen as follows: $S(0) = 2700000$, $V = 600000$, $I_n = 500000$, $T_i = 350000$, $R = 0$, $B = 500$.

4.1.1 Impact of Interventions on Treated Cases

The figure 4.1 represents the effect of different interventions strategies on the number of infected individuals that are receiving treatment over time. The green curve represents the treatment-only scenario. It has the highest peak among all strategies. This indicates that more people are getting infected, due to lack of prevention measures (WASH and vaccination), and consequently, more people get treated, which accounts for the sharp initial decline. However, overtime, the curve exhibits a flattened, extended decline. Since the rate of new infections is high, the overall number of treated cases remains relatively high for a longer period, indicating that in the long run, more time is taken to reduce the burden. This implies that without WASH or vaccination, treatment alone is less effective in controlling the disease overtime. The orange curve, which illustrates the treatment and vaccination scenario, has a slightly lower peak than the treatment-alone scenario. This is because vaccination helps in reducing the number of infections overtime, resulting in fewer people needing treatment. The

downward trend is similar to that of treatment alone, but is slightly quicker. This suggests that treatment and vaccination have some contribution to disease control. The blue curve shows the treatment-with-WASH scenario. The peak is lower than both the treatment-only and treatment-with-vaccination scenarios. WASH interventions help reduce the transmission of cholera bacteria, either through the environment or through contact with infected individuals. This leads to a lower number of infections, which results in fewer people requiring treatment overtime. The decline is also faster than the previous scenarios, suggesting that treatment and WASH are moderately effective in controlling cholera. The purple curve illustrates the WASH, treatment and vaccination scenario. This scenario shows the lowest peak among all four strategies. With both prevention measures (vaccination and WASH), the number of new infections is greatly reduced. Due to treatment, the individuals that get infected recover, and the possibility of new infections remains low. This scenario also exhibits the most substantial and sustained long-term decline, indicating that combined interventions effectively prevent new infections and reduce the overall burden of the disease. The graph shows that although all scenarios show a declining trend after the peak, the decline is more pronounced with interventions that include WASH and vaccination. Integrating vaccination and treatment with WASH is the best strategy for reducing the spread of cholera in slum settings.

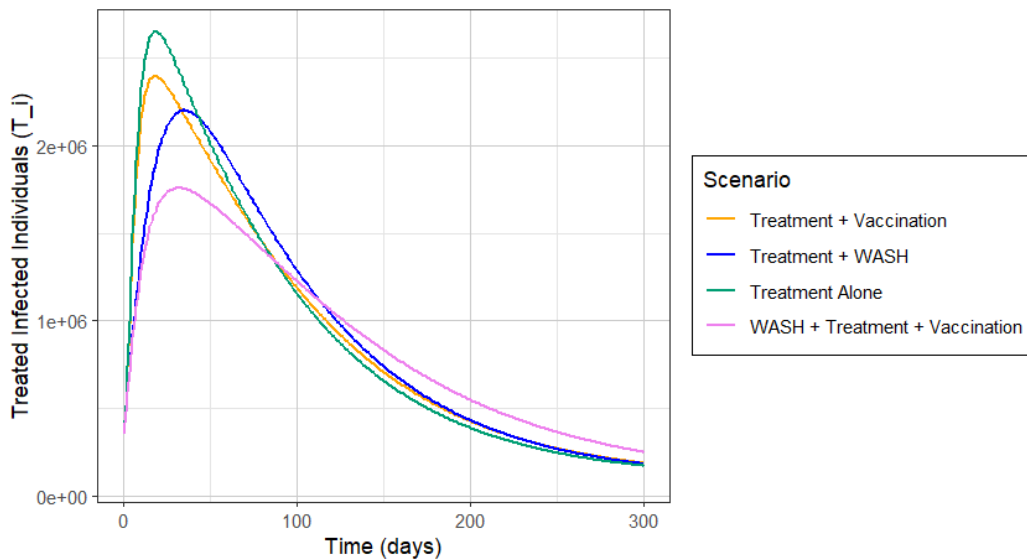


Figure 4.1: Impact of intervention strategies on T_i

4.1.2 Impact of Interventions on Untreated Treated Cases

Figure 4.2, shows the number of untreated infected individuals over time under different intervention scenarios. The orange curve, which shows the vaccination-alone scenario, exhibits the highest peak. This is because vaccination increases immunity, but it does not immediately treat individuals who are already infected. This suggests that, in the absence of WASH, vaccination alone is less effective at preventing a large number of individuals from becoming infected in the early stages of an outbreak. Overtime, more people become immune and infected individuals recover naturally, accounting for the steep decline of the peak. The green curve shows when WASH is implemented alone. The peak is lower than in the vaccination-alone scenario. Improved water, sanitation and hygiene reduces transmission by limiting exposure to contaminated environment, hence the lower number of infections. However, the peak is still significant since WASH only reduces transmission rather than increasing immunity. The reduction of cases is steady but moderately slower compared to vaccination. This is because WASH alone only lowers transmission and does not directly prevent infection. The blue curve represents the WASH-with-vaccination scenario. This combination results in the lowest peak of all the three scenarios. By integrating both interventions, transmission is reduced through WASH and immunity is enhanced through vaccination. This scenario reduces both the number of infections and the spread of the disease. The curve shows a sustained decline, indicating that overtime, the number of infections are effectively reduced. Combining WASH and vaccination is the most effective strategy for individuals who recover naturally, as it not only reduces the peak, but also accelerates their decline in the long run.

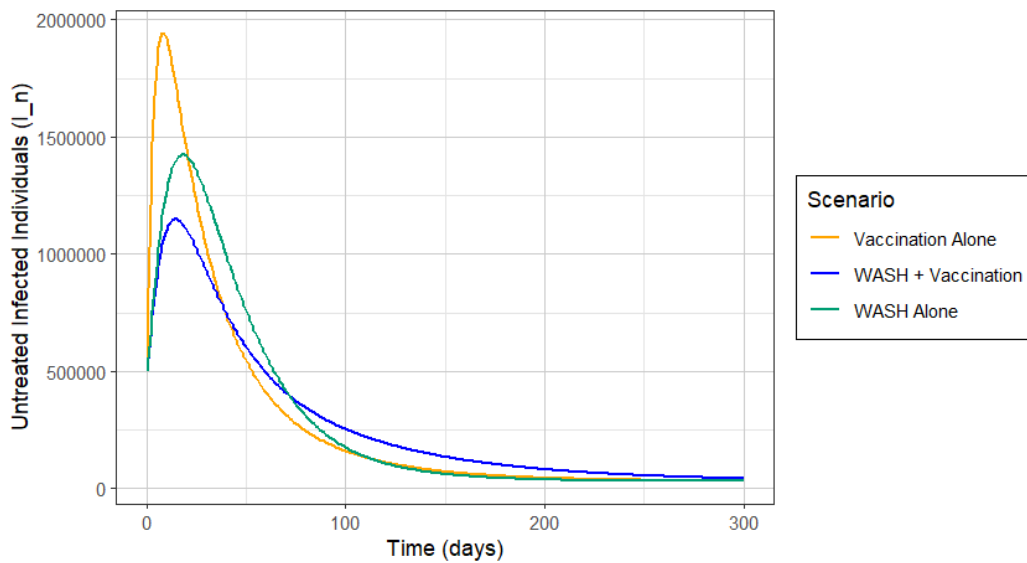


Figure 4.2: Impact of intervention strategies on I_n

4.1.3 Impact of intervention strategies on bacterial density

The graph 4.3 illustrates the bacteria concentration in the environment overtime under different intervention strategies. The blue curve shows the vaccination-with-treatment scenario. It has the highest peak. This is because vaccination reduces susceptibility of individuals but does not directly impact pathogen shedding from infected individuals. Treatment reduces the period of infection, but does not entirely prevent bacterial shedding. Due to absence of WASH intervention, like chlorination of water or waste treatment, bacteria in the environment persist for a longer time. The decline is relatively slow, this is because vaccination and treatment focus on reducing human infections but do not directly address environmental contamination. The green curve shows the WASH-only scenario. The peak is significantly reduced compared to the treatment-with-vaccination scenario. This is because WASH slows down bacterial growth by improving water, sanitation, and hygiene. The decline shows that bacteria levels approach zero more quickly, highlighting the effectiveness of WASH interventions in controlling environmental contamination. The orange curve represents the scenario in which all interventions are implemented. It has the lowest peak of bacterial density. This is because integrating all interventions reduces bacterial growth from both human

and environmental sources early in the outbreak. Treatment reduces the rate at which infected individuals contribute to bacterial shedding, vaccination increases immunity, reducing the number of infections, and WASH minimizes bacterial contamination in the environment. The curve also shows a fast decline, demonstrating the synergistic effect of combining WASH, treatment, and vaccination in controlling cholera transmission and reducing environmental contamination.

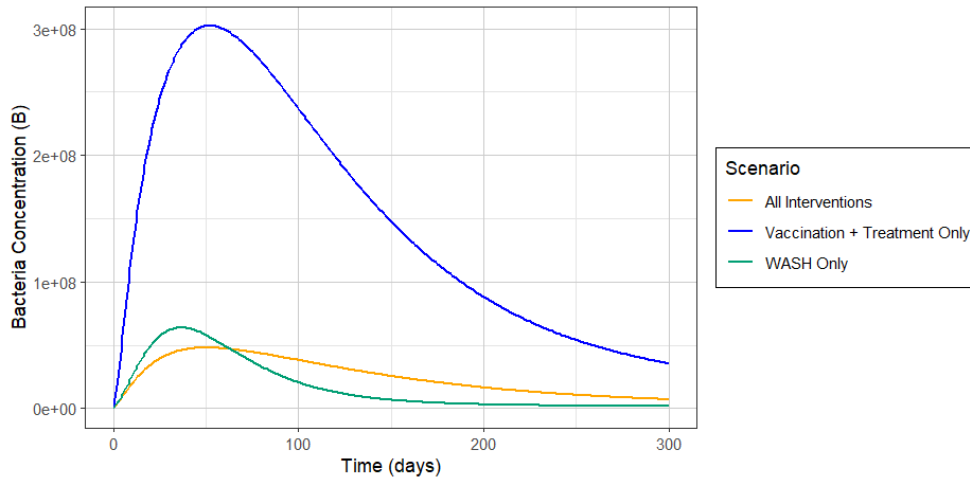


Figure 4.3: Impact of intervention strategies on B

4.1.4 Temporal Dynamics of Combined Cholera Interventions

The trajectories of the above figures (T_i , I_n and B) under the combined intervention of treatment, vaccination, and WASH exhibits a distinctive pattern. The combined strategy of treatment, vaccination, and WASH in T_i dynamics exhibits the lowest peak in cases, indicating a strong early suppression of transmission. However in the long term, it results in higher numbers of treated individuals as compared to other interventions. This is because, when combined intervention effectively reduces infections early, fewer individuals acquire natural immunity from infection, slowing the accumulation of immunity within the population. The protective effects of vaccine may also wane overtime. These factors make residual transmission persistent at low levels for an extended period, producing a prolonged epidemic tail. This similarly explains the dynamics in the I_n plot. Studies done by [Chowdhury et al. \(2023\)](#) and [Im et al. \(2024\)](#) show that the magnitude and timing of the effects of combined

WASH and vaccination strategies can differ, even though they provide better protection together than either alone.

Interventions with higher peaks may lead to quick epidemic drop due to the high build up of natural immunity since many people acquire immunity from infection. This leads to lower number of cases in the long run. These findings illustrate a trade-off between immediate epidemic suppression and long-term transmission dynamics. They are crucial for designing sustainable cholera control programs that balance short-term impact with long-term disease management.

4.2 Optimal Control Analysis of WASH Interventions

Numerical simulations conducted on the control system (3.26) are run in R using the forward backward sweep method based on the fourth-order Runge-Kutta method. The iterative process updates the control variables while alternately solving the state equations forward in time and the adjoint equations backward in time, ensuring convergence to an optimal control trajectory. Parameters used are provided in table 3.2. The parameters were obtained from different literature and whenever they are not available or are not estimated, theoretical assumptions within realistic ranges are made in order to carry out graphical illustrations.

4.2.1 Impact of Individual WASH Intervention

Here, the effect of one active control at a time is used to optimize the objective function (3.25), while the rest of the controls are kept at zero. The initial state conditions are chosen as $S(0) = 270000$, $V = 50000$, $I_n = 100000$, $T_i = 50000$, $R = 0$, $B = 500$ and initial conditions for the weight constants as $C_4 = 50$, $C_5 = 50$, $C_6 = 50$ and $C_4 = 30$ for T_i , $C_4 = 10$, $C_5 = 10$, $C_6 = 10$ and $C_4 = 10$ for I_n , and $C_4 = 50$, $C_5 = 50$, $C_6 = 50$, $C_4 = 30$ for B .

Effect of Individual WASH Interventions on T_i

These graphs display the effect of different WASH interventions on the number of infected individuals in the treated compartment (T_i) over time. The individuals when no WASH interventions are employed are represented by the solid line and those when there is an intervention are represented by the dotted line. In the first plot, the impact of environmental pathogen concentration on transmission is assessed. ω_1 controls environmental transmission by reducing bacteria exposure through improved water quality. The graph for ω_1 , represented by the dotted blue line, shows a moderate peak showing that the intervention reduces peak infections, and steady decline indicating that reducing environmental transmission can effectively control the spread of cholera.. Initially the number of infected individual rises since the epidemic is still developing. However, as the intervention takes effect, environmental contamination is reduced, causing the epidemic to slow down. This accounts for the decline in cases compared to the no-intervention scenario. The graph for ω_2 shows the impact on human-to-human transmission. ω_2 decreases direct human-to-human transmission rates through hygiene such as handwashing and improved sanitation facilities. The graph displays minimal impact as the intervention curve closely follows the no-control curve. This suggests that while hygiene measures reduce spread due to human contact, it does not significantly change the outbreak's trajectory without other interventions. The graph for ω_3 shows the dynamics when bacterial shedding is controlled, reducing the contribution of infected individuals to environmental contamination. This intervention leads to a significant decline in peak infections and a sharp early drop, indicating a strong early effect.. The last graph shows the impact on bacteria decay rate. ω_4 enhances the decay of bacteria in the environment by improving waste management. The number of infected individuals are significantly lowered but it is a weaker effect as compared to ω_1 and ω_3 , since the control curve and the no-control curve are close. This shows a need for a combined effort, even though increasing bacteria decay rate helps.

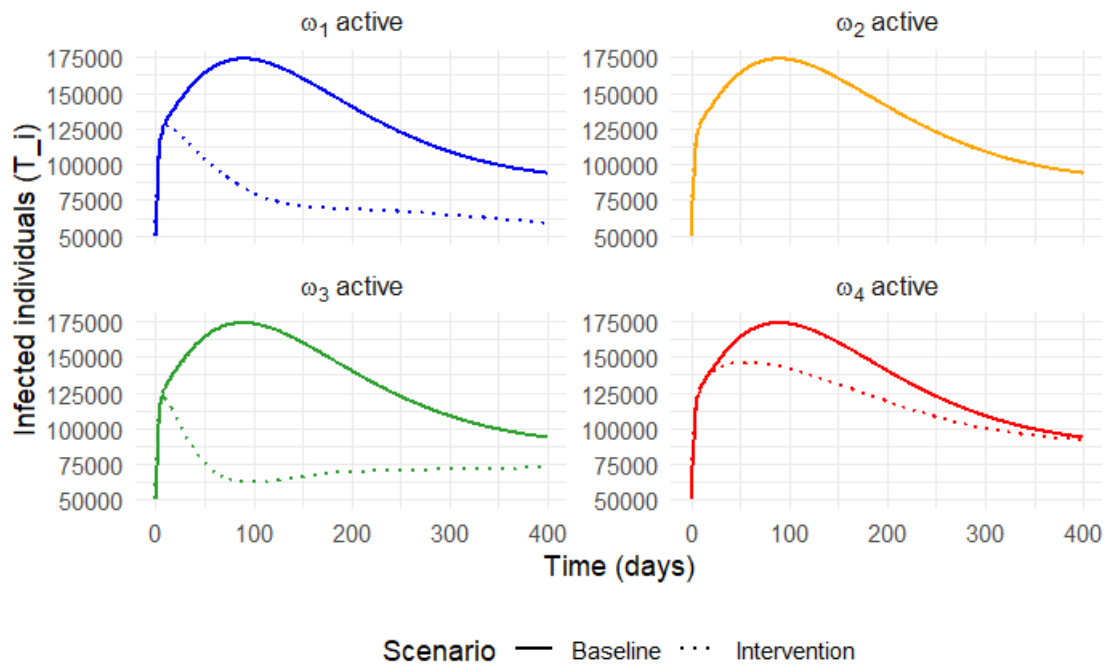


Figure 4.4: Impact of individual WASH intervention on T_i . The control parameters ω_1 to ω_4 represent reduction of environmental contamination, reduction of human-to-human transmission, reduction of pathogen shedding by infected individuals, and acceleration of environmental pathogen decay, respectively. Each subplot compares the intervention scenario to the no-intervention baseline.

Effect of Individual WASH Interventions on I_n

The graphs compare the impact of different WASH interventions on the number of untreated infected individuals I_n over time. In the first plot, the number of infected individuals is lower than that of the no WASH intervention scenario. With the intervention, there is a sharper initial decline, leading to a lower steady-state level. The plot shows that long-term, non-treated infections remain substantially lower when environmental transmission is reduced compared to the baseline curve. This suggests that preventing contamination of water sources has a strong persistent effect on reducing untreated cases. In ω_2 subplot, the dotted line (intervention scenario) almost entirely overlaps the solid line (baseline), indicating that reducing direct contact transmission had a negligible effect on the untreated infected. This indicates that under the given model structure and parameter settings, WASH interventions

focused solely on reducing direct contact transmission are not sufficient to lower the burden of untreated cholera cases. The third plot shows a sharp decline in both scenarios, but ω_3 achieves a significantly lower prevalence. Bacterial shedding contributes directly to environmental contamination and secondary transmission, and reducing this has a strong indirect effect on untreated cases. This indicates the crucial role of reducing contamination from infected individuals. The ω_4 intervention reduces infections, but is not as effective as ω_1 and ω_3 . From the plots, it is clear that interventions with ω_1 and ω_3 are effective in reducing the spread of the disease. ω_2 is the least effective when applied alone.

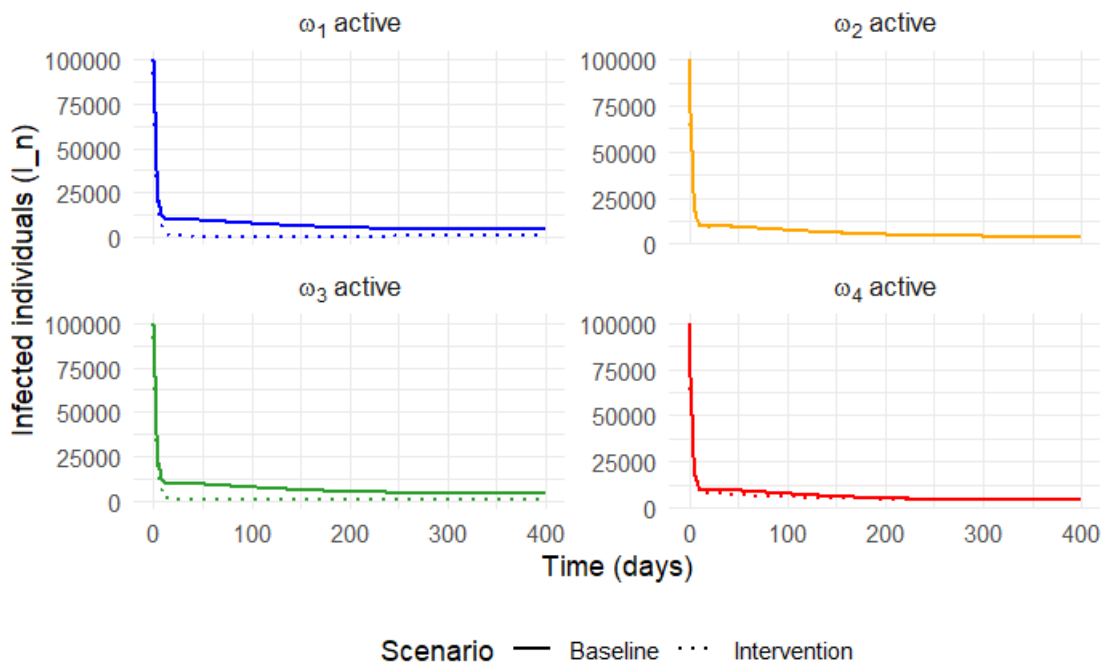


Figure 4.5: Impact of individual WASH intervention on I_n . The control parameters ω_1 to ω_4 represent reduction of environmental contamination, reduction of human-to-human transmission, reduction of pathogen shedding by infected individuals, and acceleration of environmental pathogen decay, respectively. Each subplot compares the intervention scenario to the no-intervention baseline.

Effect of Individual WASH Interventions on Pathogen Concentration (B)

The graphs compare the impact of different WASH interventions on bacterial density over time. In terms of peak reduction of bacterial density, ω_1 shows a moderate effect. The plot

indicates that reducing environmental transmission helps limit exposure but does not directly reduce bacterial shedding or presence. On the other hand, the curve for ω_2 overlaps with the baseline curve. This is because ω_2 has no impact on the density of bacteria as it primarily targets transmission rather than environmental contamination. The ω_3 intervention has the most impact in decreasing the peak, since reducing pathogen shedding by infected individuals helps prevent environmental contamination. Since shedding fuels the pathogen reservoir, controlling it significantly reduces bacterial growth. Similarly, ω_4 intervention, which increases bacterial decay portrays a significant reduction in peak bacterial density, although less proactive than ω_3 . This suggests that lessening shedding from infected individuals is the most effective intervention, followed by environmental pathogen removal.

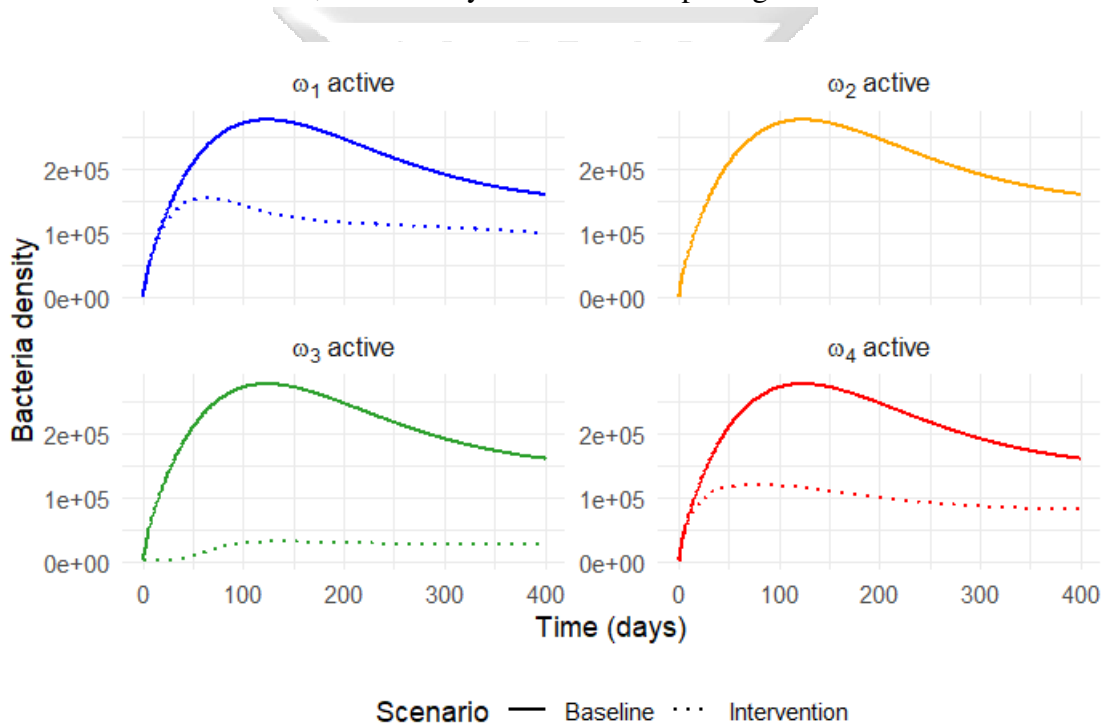


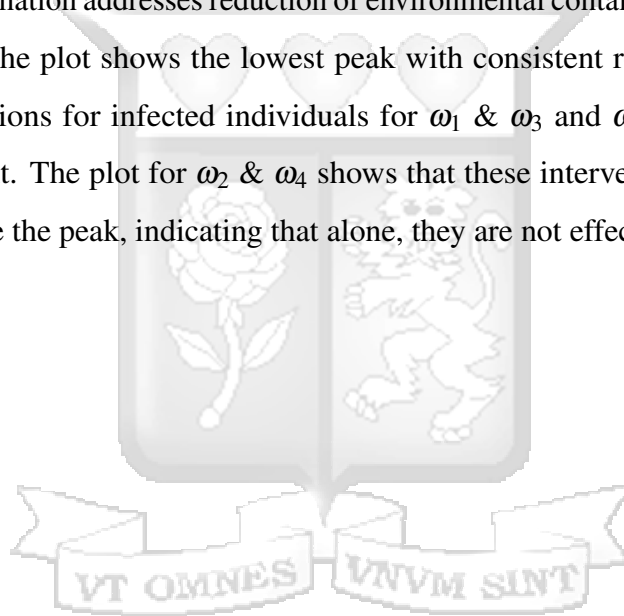
Figure 4.6: Impact of individual WASH intervention on B . The control parameters ω_1 to ω_4 represent reduction of environmental contamination, reduction of human-to-human transmission, reduction of pathogen shedding by infected individuals, and acceleration of environmental pathogen decay, respectively. Each subplot compares the intervention scenario to the no-intervention baseline.

4.2.2 Effects of Two Distinct Combined WASH Interventions

The graphs illustrate the effect of combining two WASH interventions. The initial state conditions are chosen as $S(0) = 270000$, $V = 50000$, $I_n = 100000$, $T_i = 10000$, $R = 0$, $B = 500$ and initial conditions for the weight constants as $C_4 = 50$, $C_5 = 50$, $C_6 = 50$ and $C_4 = 30$ for T_i , $C_4 = 10$, $C_5 = 10$, $C_6 = 10$ and $C_4 = 10$ for I_n , and $C_4 = 50$, $C_5 = 50$, $C_6 = 50$ and $C_4 = 30$ for B .

Effect of Two Combined WASH Interventions on T_i

The ω_1 & ω_4 combination addresses reduction of environmental contamination with increased pathogen decay. The plot shows the lowest peak with consistent reductions in T_i . There is moderate reductions for infected individuals for ω_1 & ω_3 and ω_3 & ω_4 , but the ω_1 & ω_4 is more efficient. The plot for ω_2 & ω_4 shows that these interventions together do not significantly reduce the peak, indicating that alone, they are not effective enough.



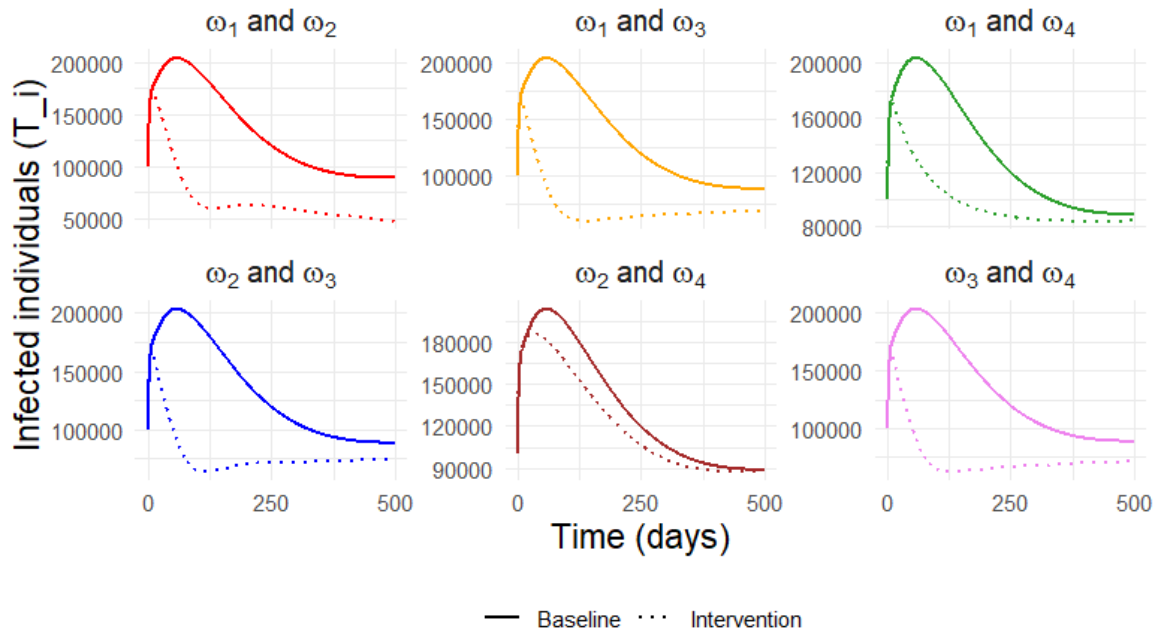


Figure 4.7: Impact of 2 WASH interventions on T_i . The control parameters ω_1 to ω_4 represent reduction of environmental contamination, reduction of human-to-human transmission, reduction of pathogen shedding by infected individuals, and acceleration of environmental pathogen decay, respectively. Each subplot compares the intervention scenario to the no-intervention baseline.

Effect of Two Combined WASH Interventions on I_n

The graph displays the effect of two WASH strategies on the number of infected untreated individuals. The plots for ω_1 & ω_2 , ω_1 & ω_3 , ω_1 & ω_4 , ω_2 & ω_3 and ω_3 & ω_4 show significant and rapid drop of cases especially in the early outbreak days. ω_2 & ω_4 show almost no change with the no-control curve implying that they are less effective and take longer to fully control infections of the untreated cases.

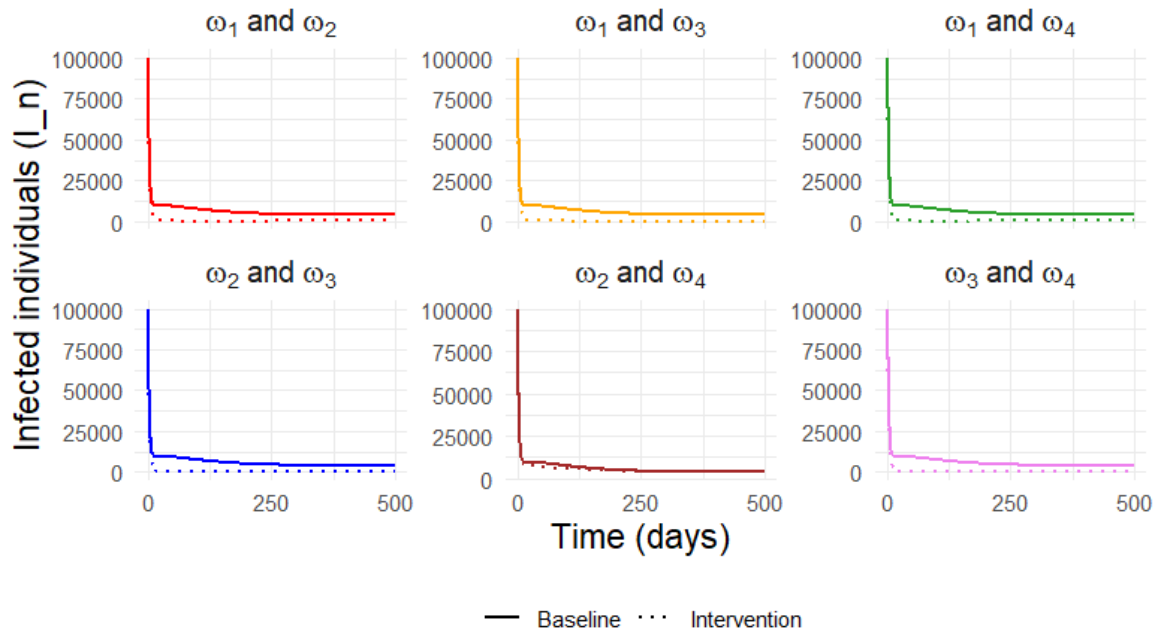


Figure 4.8: Impact of 2 WASH interventions on I_n . The control parameters ω_1 to ω_4 represent reduction of environmental contamination, reduction of human-to-human transmission, reduction of pathogen shedding by infected individuals, and acceleration of environmental pathogen decay, respectively. Each subplot compares the intervention scenario to the no-intervention baseline.

Effect of Two Combined WASH Interventions on B

In terms of peak reductions, all interventions significantly reduce the peak of the bacteria density. However ω_3 & ω_4 shows the lowest bacteria peak, with the strongest suppression. The bacteria levels plateaus at a low level, indicating a balanced input-output where shedding is minimized and decay maximized. In the ω_1 & ω_2 subplot, the bacteria decline overtime, but remain at a relatively elevated steady-state. This indicates that without sanitation or decay acceleration, bacteria persists in the environment. The subplots ω_1 & ω_3 and ω_2 & ω_3 have a sharp suppression of the bacteria peak, but post-peak, the bacteria levels stabilizes. This suggests that although these interventions help, the absence of direct environmental measures (ω_1 and ω_4) limits further reduction. ω_1 & ω_4 shows a significant impact in reducing both

the peak and long-term bacteria levels. ω_2 & ω_4 shows a moderate peak reduction and a continuous decrease over time.

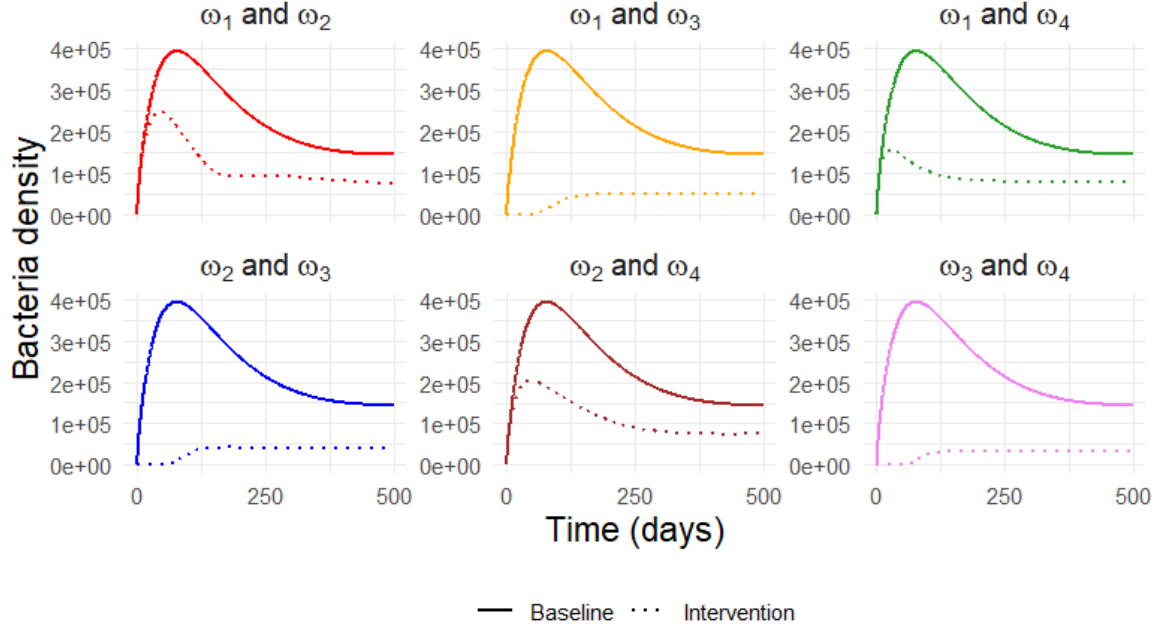
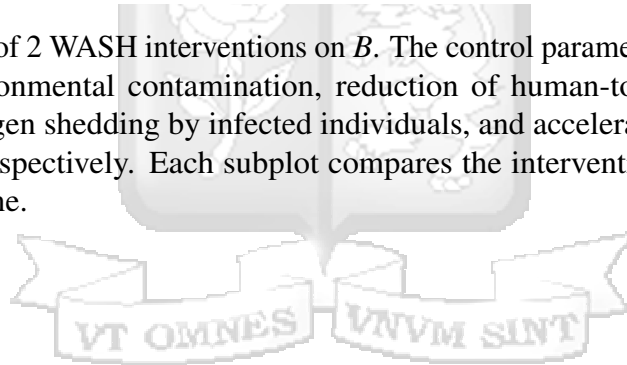


Figure 4.9: Impact of 2 WASH interventions on B . The control parameters ω_1 to ω_4 represent reduction of environmental contamination, reduction of human-to-human transmission, reduction of pathogen shedding by infected individuals, and acceleration of environmental pathogen decay, respectively. Each subplot compares the intervention scenario to the no-intervention baseline.



4.2.3 Impact of Three Different Combined WASH Interventions

The figures here show the impact of combining all four WASH interventions in the first subplot, and three WASH interventions active in each of the other three subplots. The initial state conditions are chosen as $S(0) = 2500000$, $V = 50000$, $I_n = 100000$, $T_i = 50$, $R = 0$, $B = 500$ for T_i and B , $S(0) = 2700000$, $V = 50000$, $I_n = 100000$, $T_i = 50000$, $R = 0$, $B = 500$ for I_n and initial conditions for the weight constants as $C_4 = 500$, $C_5 = 10$, $C_6 = 500$ and $C_4 = 10$ for T_i , $C_4 = 10$, $C_5 = 10$, $C_6 = 10$ and $C_4 = 10$ for I_n , and $C_4 = 500$, $C_5 = 10$, $C_6 = 500$ and $C_4 = 10$ for B .

Effect of Different Combined WASH Interventions on T_i

When all interventions are active, we have the lowest infection peak. This is displayed in the second plot. The rate at which infection declines is faster in the plots for ω_1 & ω_3 & ω_4 and ω_2 & ω_3 & ω_4 as compared to ω_1 & ω_2 & ω_3 . This illustrates that for long-time control of cholera infections in treated individuals, all four interventions are recommended, the second best strategy being ω_1 & ω_3 & ω_4 and ω_2 & ω_3 & ω_4 .

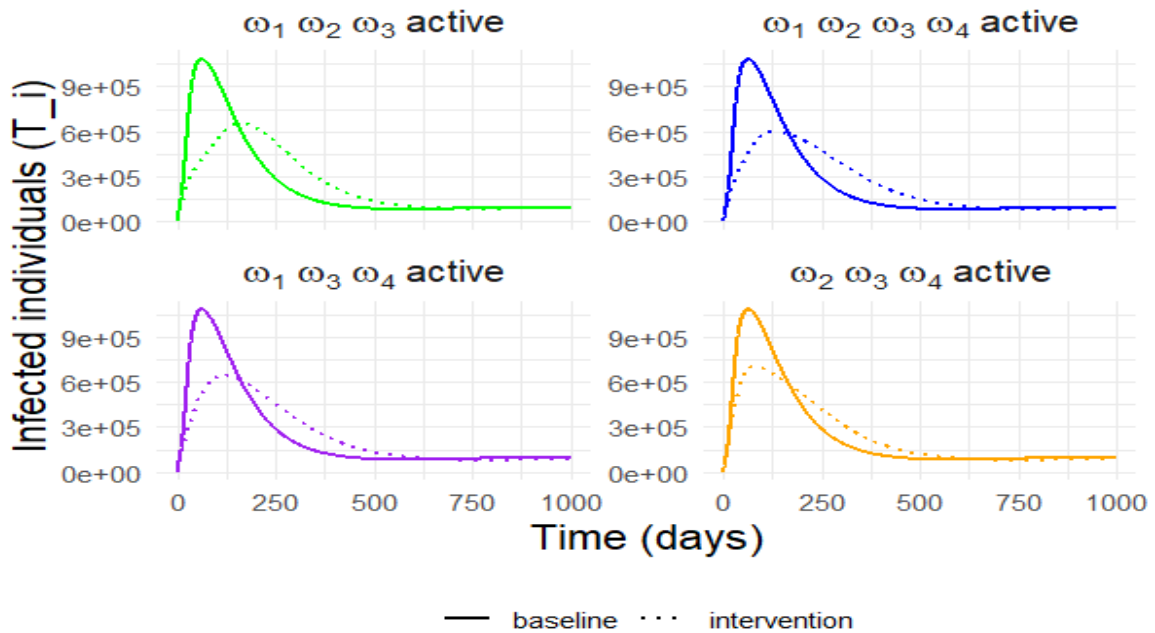


Figure 4.10: Impact of different WASH interventions on T_i . The control parameters ω_1 to ω_4 represent reduction of environmental contamination, reduction of human-to-human transmission, reduction of pathogen shedding by infected individuals, and acceleration of environmental pathogen decay, respectively. Each subplot compares the intervention scenario to the no-intervention baseline.

Effect of Different Combined WASH Interventions on I_n

All interventions shows a substantial drop in infected individuals compared to the no intervention curve. This shows that when three or more interventions are implemented, there is a strong synergistic effect in minimizing the number of untreated cases. The second plot shows the largest reduced number of untreated infected individuals.

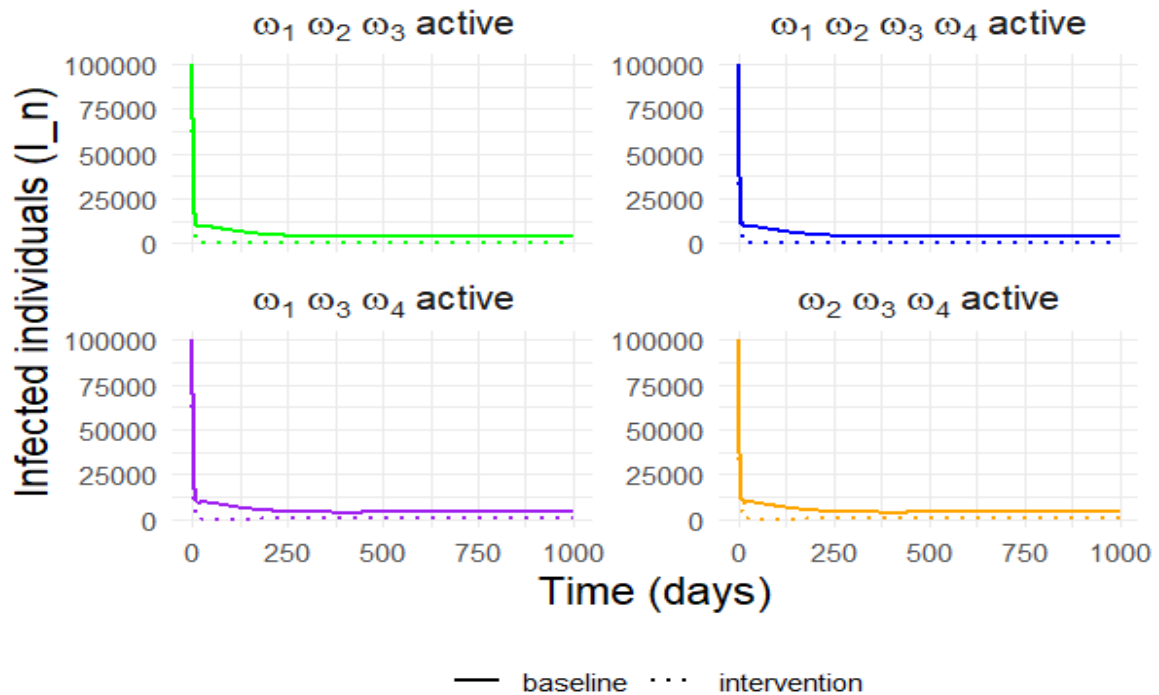


Figure 4.11: Impact of different WASH interventions on I_n . The control parameters ω_1 to ω_4 represent reduction of environmental contamination, reduction of human-to-human transmission, reduction of pathogen shedding by infected individuals, and acceleration of environmental pathogen decay, respectively. Each subplot compares the intervention scenario to the no-intervention baseline.

Effect of Different Combined WASH Interventions on B

The graph examines the impact of various WASH interventions on the bacteria density in the environment overtime. In all of the subplots, there is a significant reduction of peak showing effectiveness of all the interventions combined. However, the first plot has the lowest bacteria peak indicating the highest effect when all interventions are implemented. The second subplot with ω_1 & ω_2 & ω_3 WASH interventions shows the highest peak with the slowest decline of bacteria density and longest outbreak period. We note that this subplot does not include ω_4 as one of the WASH intervention, implying that for long-term eradication of bacteria, the WASH intervention that increases the decay of bacteria is essential.

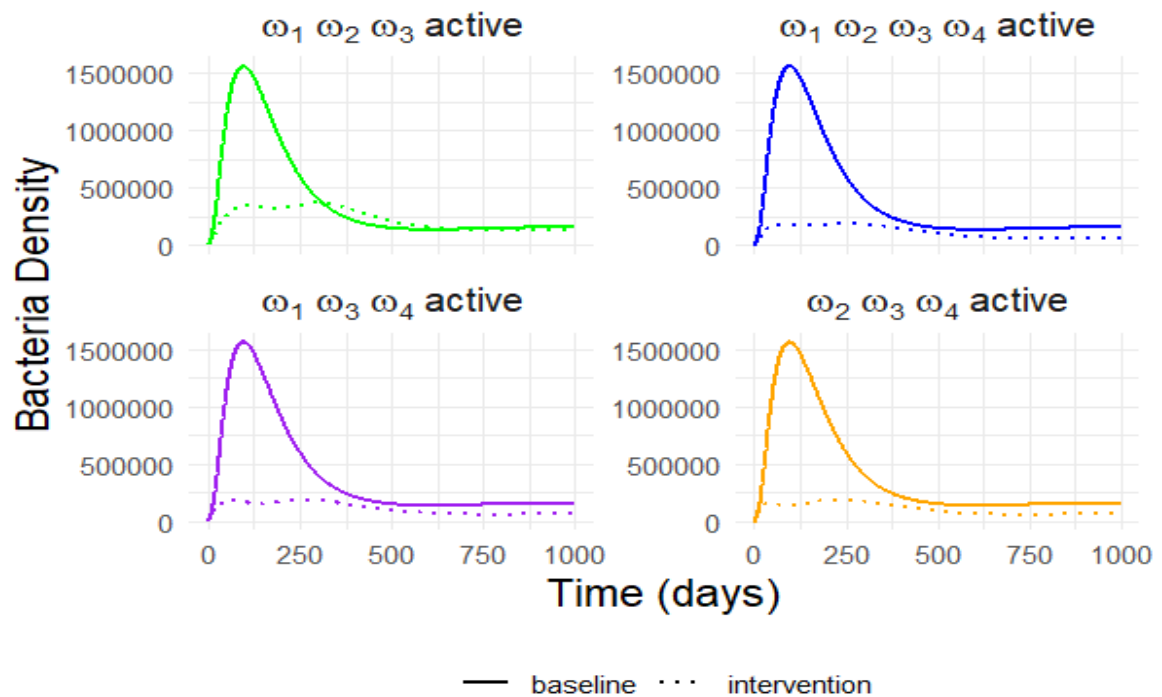
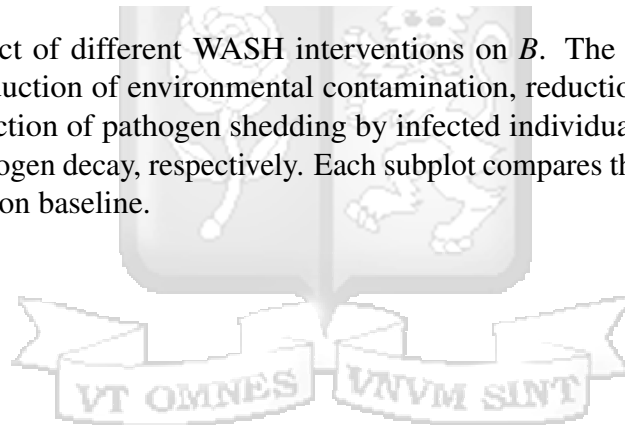


Figure 4.12: Impact of different WASH interventions on B . The control parameters ω_1 to ω_4 represent reduction of environmental contamination, reduction of human-to-human transmission, reduction of pathogen shedding by infected individuals, and acceleration of environmental pathogen decay, respectively. Each subplot compares the intervention scenario to the no-intervention baseline.



Chapter 5

Conclusion and Recommendation

5.1 Conclusion and Recommendation

This research examined the dynamics of cholera transmission in Nairobi slums through a mathematical model that incorporated vaccination, treatment and WASH interventions. The existence of local and global stability for the disease free equilibrium was established. Sensitivity analysis was conducted and it was determined that some parameters had a significant influence on the spread of cholera when compared to others. The deterministic model was used to run simulations to assess the effect vaccination and treatment both in the presence and absence of enhanced WASH. This was done through scenario analysis. It was observed that the WASH-with-vaccination scenario resulted in the lowest number of untreated infected individuals, indicating that WASH interventions significantly reduce exposure to the pathogen. The bacterial density was lowest in scenarios that included WASH, confirming its role in reducing environmental contamination and minimizing transmission. The treated infected individuals curve showed that treatment alone can quickly reduce the number of severe cases but does not prevent new infections, leading to a continuous cycle of reinfection. The bacterial load remained high in the vaccination-with-treatment scenario, indicating that medical interventions without WASH do not eliminate bacteria in the environment. The scenario incorporating all interventions resulted in the lowest peak of infected individuals and the fastest reduction in bacterial concentration. In particular, the combination of WASH and vaccination proved effective in reducing both cholera cases and bacterial persistence.

This study also used the optimal control approach to examine the impact of WASH interventions on the dynamics of cholera spread. In resource-limited settings, and slums that require a particular intervention, the results offer valuable insights for decision making. The

analysis included strategies with individual interventions, combinations of two and three interventions, and integration of all the WASH interventions. For individual interventions, sanitation improvement such as toilets (ω_3), followed by water treatment (ω_1) were the most effective standalone interventions for reducing the number of infections. The bacteria load was greatly impacted by waste management (ω_4) and sanitation improvement (ω_3), suggesting that overall in cases where only one intervention is achievable, priority should be given to sanitation (ω_3). For the two-intervention strategies, water treatment (ω_1) and waste management (ω_4) were the most effective combinations, significantly reducing infection rates. Hand hygiene (ω_2) was less effective when paired with either water treatment (ω_1), improved sanitation and fecal sludge management (ω_3), or wastewater treatment (ω_4). Reduction of bacterial density was highest when improved sanitation and fecal sludge management (ω_3) was paired with wastewater treatment (ω_4).

When three WASH interventions were integrated, cholera control was further enhanced by reducing both peak infection levels and environmental bacterial load more significantly than two-intervention approaches. Water treatment (ω_1), improved sanitation and fecal sludge management (ω_3) and waste management (ω_4) was the most effective three-intervention strategy, significantly reducing cholera prevalence and bacterial density. Hand hygiene (ω_2), improved sanitation (ω_3) and waste management (ω_4) combination was the second best and most beneficial in areas with poor waste disposal and open defecation. The full combination of water treatment, sanitation, hygiene, and waste management yielded the greatest impact, minimizing bacterial load, reducing peak infections, and shortening epidemic duration.

Based on these findings, if only one WASH intervention is feasible, improved sanitation and safe fecal sludge management, or water treatment should be prioritized. If two interventions can be implemented, water treatment and waste management should be preferred, followed by hand hygiene and hygienic practices in food handling with sanitation infrastructure. If resources accede three WASH interventions, the first course of action should be water treatment, improved sanitation and fecal sludge management and waste management. In regards to targeted WASH strategies for those slums with different conditions, water treatment and improved sanitation should be implemented in slums with weak accessibility to safe water in

order to reduce direct transmission. In areas with poor waste disposal, sanitation, hygiene promotion and waste management should be stressed. Lastly, In densely populated slums with open defecation concerns improved sanitation and waste management should be emphasized to reduce fecal-oral transmission routes. Hygienic practices such as hand washing and safe practices in food handling should much rather complement other WASH interventions in comparison to being stand alone. While single and partial strategies help to control the spread of cholera, the greatest reduction occurs when all interventions are applied together. This study provides an understanding of how cholera can be controlled through multiple control strategies in order to combat the transmission of the disease. It will help policymakers and stakeholders in working towards progressive implementation of all interventions and community-driven education of sanitation and hygiene to sustain intervention benefits. Results from this study will allow efficient allocation of resources, ensuring sustainable and effective cholera prevention strategies in vulnerable urban populations. This work will also provide a useful reference for researchers doing further studies on multiple control strategies for cholera control. In future, studies should consider the influence of climate change and socioeconomic factors on the dynamics of cholera transmission. To enhance policy applicability, utilization of real time data to parameterize the model developed, and field validation of the model predictions should be pursued.



References

- Abdulrahim, A. and Adesola, R. O. (2022). Antimicrobial resistance in cholera: a need for quick intervention in Nigeria, West Africa. *International Journal of Travel Medicine and Global Health*, 10(3):99–103.
- Abera, B., Bezabih, B., and Dessie, A. (2010). Antimicrobial susceptibility of *v. cholerae* in north west, Ethiopia. *Ethiopian Medical Journal*, 48(1):23–8.
- Anderson, R. M. (2013). *The population dynamics of infectious diseases: theory and applications*. Springer.
- Anis, H., Uwishema, O., Hamitoglu, A. E., Essayli, D., El Kassem, S., Rogose, M. S., Al Maaz, Z., and Nazir, A. (2023). Multicountry cholera outbreak alert in Kenya: Current efforts and recommendations. *International Journal of Surgery*, 109(3):555–557.
- Awofeso, N. and Aldbak, K. (2018). Cholera, migration, and global health—a critical review. *International Journal of Travel Medicine and Global Health*, 6(3):92–99.
- Ayoade, A., OJ, I. M. P., and Oguntolu, F. (2018). A mathematical model on cholera dynamics with prevention and control. *Covenant Journal of Physical and life sciences*.
- Bakare, E. A. and Hoskova-Mayerova, S. (2021). Optimal control analysis of cholera dynamics in the presence of asymptotic transmission. *Axioms*, 10(2):60.
- Barratt, H., Kirwan, M., and Shantikumar, S. (2018). Epidemic theory (effective & basic reproduction numbers, epidemic thresholds) & techniques for analysis of infectious disease data (construction & use of epidemic curves, generation numbers, exceptional reporting & identification of significant clusters). *Health Knowledge*.
- Bhattacharya, S. K. (2003). An evaluation of current cholera treatment. *Expert opinion on pharmacotherapy*, 4(2):141–146.
- Brauer, F., Castillo-Chavez, C., Feng, Z., et al. (2019). *Mathematical models in epidemiology*, volume 32. Springer.
- Bwire, G., Munier, A., Ouedraogo, I., Heyerdahl, L., Komakech, H., Kagirita, A., Wood, R., Mhlanga, R., Njanpop-Lafourcade, B., Malimbo, M., et al. (2017). Epidemiology of cholera outbreaks and socio-economic characteristics of the communities in the fishing villages of Uganda: 2011-2015. *PLoS neglected tropical diseases*, 11(3):e0005407.
- Cairncross, S., Hunt, C., Boisson, S., Bostoen, K., Curtis, V., Fung, I. C., and Schmidt, W.-P. (2010). Water, sanitation and hygiene for the prevention of diarrhoea. *International journal of epidemiology*, 39(suppl_1):i193–i205.
- Carpenter, C. (1971). Cholera: diagnosis and treatment. *Bulletin of the New York Academy of Medicine*, 47(10):1192.

- Cheng, K.-C. (2024). Cholera, an old foe, is becoming a new kind of problem for Kenya. Accessed on August 2024. Link: [www.gavi.org/vaccineswork/cholera-old-foe-becoming-new-kind-problem-kenya#:~:text=cholera%20transmission%20increase.-,According%20to%20the%20World%20Health%20Organization%20\(WHO\)%2C%20Kenya%20has,case%20fatality%20rate%20of%201.7%25](http://www.gavi.org/vaccineswork/cholera-old-foe-becoming-new-kind-problem-kenya#:~:text=cholera%20transmission%20increase.-,According%20to%20the%20World%20Health%20Organization%20(WHO)%2C%20Kenya%20has,case%20fatality%20rate%20of%201.7%25).
- Chowdhury, F., Aziz, A. B., Ahmmed, F., Ahmed, T., Kang, S. S., Im, J., Park, J., Tadesse, B. T., Islam, M. T., Kim, D. R., et al. (2023). The interplay between wash practices and vaccination with oral cholera vaccines in protecting against cholera in urban Bangladesh: reanalysis of a cluster-randomized trial. *Vaccine*, 41(14):2368–2375.
- Chowdhury, F., Ross, A. G., Islam, M. T., McMillan, N. A., and Qadri, F. (2022). Diagnosis, management, and future control of cholera. *Clinical Microbiology Reviews*, 35(3):211–221.
- Citaristi, I. (2022). United nations human settlements programme—un-habitat. In *The Europa Directory of International Organizations 2022*, pages 240–243. Routledge.
- Codeço, C. T. (2001). Endemic and epidemic dynamics of cholera: the role of the aquatic reservoir. *BMC Infectious diseases*, 1:1–14.
- Cui, J. a., Wu, Z., and Zhou, X. (2014). Mathematical analysis of a cholera model with vaccination. *Journal of Applied Mathematics*, 2014(1):324767.
- Dowdle, W. R. (2023). The principles of disease elimination and eradication. Accessed on December 2024. Link: <https://www.cdc.gov/mmwr/preview/mmwrhtml/su48a7.htm>.
- Dumont, Y., Chiroleu, F., and Domerg, C. (2008). On a temporal model for the chikungunya disease: modeling, theory and numerics. *Mathematical Biosciences*, 213(1):80–91.
- D’Mello-Guyett, L., Gallandat, K., Van den Bergh, R., Taylor, D., Bulit, G., Legros, D., Maes, P., Checchi, F., and Cumming, O. (2020). Prevention and control of cholera with household and community water, sanitation and hygiene (WASH) interventions: a scoping review of current international guidelines. *PLoS One*, 15(1):e0226549.
- Edward, S. and Nyerere, N. (2015). A mathematical model for the dynamics of cholera with control measures. *Applied and computational Mathematics*, 4(2):53–63.
- Fung, I. C.-H. (2014). Cholera transmission dynamic models for public health practitioners. *Emerging Themes in Epidemiology*, 11:1–11.
- GTFCC (2018). Technical note: Use of antibiotics for the treatment and control of cholera [internet]. 2018.gtfcc case management working group and others. Accessed on August 2024. Link: www.gtfcc.org/wp-content/uploads/2019/10/gtfcc-technical-note-on-use-of-antibiotics-for-the-treatment-of-cholera.pdf.
- Hartley, D. M., Morris Jr, J. G., and Smith, D. L. (2006). Hyperinfectivity: a critical element in the ability of *v. cholerae* to cause epidemics? *PLoS medicine*, 3(1):e7.
- Im, J., Islam, M. T., Ahmmed, F., Kim, D. R., Tadesse, B. T., Kang, S., Khanam, F., Chowdhury, F., Ahmed, T., Firoj, M. G., et al. (2024). Do oral cholera vaccine and water, sanitation, and hygiene combine to provide greater protection against cholera? results from a cluster-randomized trial of oral cholera vaccine in Kolkata, India. In *Open Forum Infectious Diseases*, volume 11, page ofad701. Oxford University Press US.

- Jutla, A., Whitcombe, E., Hasan, N., Haley, B., Akanda, A., Huq, A., Alam, M., Sack, R. B., and Colwell, R. (2013). Environmental factors influencing epidemic cholera. *The American Journal of Tropical Medicine and Hygiene*, 89(3):597.
- Kamau, N. and Njiru, H. (2018). Water, sanitation and hygiene situation in Kenya's urban slums. *Journal of Health Care for the Poor and Underserved*, 29(1):321–336.
- Kiama, C., Okunga, E., Muange, A., Marwanga, D., Langat, D., Kuria, F., Amoth, P., Were, I., Gachohi, J., Ganda, N., et al. (2023). Mapping of cholera hotspots in Kenya using epidemiologic and water, sanitation, and hygiene (WASH) indicators as part of Kenya's new 2022–2030 cholera elimination plan. *PLOS Neglected Tropical Diseases*, 17(3):e0011166.
- Kim, J., Hagen, E., Muindi, Z., Mbonglou, G., and Laituri, M. (2022). An examination of water, sanitation, and hygiene (wash) accessibility and opportunity in urban informal settlements during the COVID-19 pandemic: Evidence from Nairobi, Kenya. *Science of the Total Environment*, 823:153398.
- Kobe, J., Pritchard, N., Short, Z., Erovenko, I. V., Rychtář, J., and Rowell, J. T. (2018). A game-theoretic model of cholera with optimal personal protection strategies. *Bulletin of Mathematical Biology*, 80:2580–2599.
- Kuddus, M. A., Rahman, A., Alam, F., and Mohiuddin, M. (2023). Analysis of the different interventions scenario for programmatic measles control in bangladesh: A modelling study. *PLoS One*, 18(6):e0283082.
- Mageto, L. M., Nyamai, M., Aboge, G. O., Gathura, P., Okunga, E., Muange, A., Mbae, C., Thumbi, S. M., and Kariuki, S. (2023). Spatial and temporal analysis of cholera cases in high-risk areas of Kenya. *medRxiv*, pages 2023–10.
- Maliki, O. S. and Chibuike, O. C. (2021). A mathematical model for the control of cholera epidemic without natural recovery. *Applied Mathematics*, 12(08):655–668.
- Manaseh, B. A., John, G., Simon, K., and Christine, M. (2023). Mapping cholera risk in Nairobi county, Kenya: a comprehensive analysis of environmental, socio-economic, and WASH factors. *African Journal of Health Sciences*, 36(3):286–298.
- Marwa, Y. M., Mwalili, S., and Mbalawata, I. S. (2018). Markov chain monte carlo analysis of cholera epidemic. *Journal of Mathematical and Computational Science*, 8(5):584–610.
- Mukandavire, Z., Liao, S., Wang, J., Gaff, H., Smith, D. L., and Morris Jr, J. G. (2011). Estimating the reproductive numbers for the 2008–2009 cholera outbreaks in Zimbabwe. *Proceedings of the National Academy of Sciences*, 108(21):8767–8772.
- Njagarah, J. B. H. and Nyabadza, F. (2014). A metapopulation model for cholera transmission dynamics between communities linked by migration. *Applied Mathematics and Computation*, 241:317–331.
- Onuorah, M. O., Atiku, F., and Juuko, H. (2022). Mathematical model for prevention and control of cholera transmission in a variable population. *Research in Mathematics*, 9(1):2018779.

- Phan, T. A., Tian, J. P., and Wang, B. (2021). Dynamics of cholera epidemic models in fluctuating environments. *Stochastics and Dynamics*, 21(02):2150011.
- Posny, D. and Wang, J. (2014). Modelling cholera in periodic environments. *Journal of Biological Dynamics*, 8(1):1–19.
- Saltelli, A., Tarantola, S., and Campolongo, F. (2000). Sensitivity analysis as an ingredient of modeling. *Statistical Science*, pages 377–395.
- Shaikh, H., Lynch, J., Kim, J., and Excler, J.-L. (2020). Current and future cholera vaccines. *Vaccine*, 38:A118–A126.
- Sun, G.-Q., Xie, J.-H., Huang, S.-H., Jin, Z., Li, M.-T., and Liu, L. (2017). Transmission dynamics of cholera: Mathematical modeling and control strategies. *Communications in Nonlinear Science and Numerical Simulation*, 45:235–244.
- Taylor, D. L., Kahawita, T. M., Cairncross, S., and Ensink, J. H. (2015). The impact of water, sanitation and hygiene interventions to control cholera: a systematic review. *PLoS one*, 10(8):e0135676.
- Tien, J. H. and Earn, D. J. (2010). Multiple transmission pathways and disease dynamics in a waterborne pathogen model. *Bulletin of Mathematical Biology*, 72:1506–1533.
- Tuite, A. R., Tien, J., Eisenberg, M., Earn, D. J., Ma, J., and Fisman, D. N. (2011). Cholera epidemic in Haiti, 2010: using a transmission model to explain spatial spread of disease and identify optimal control interventions. *Annals of Internal Medicine*, 154(9):593–601.
- UNICEF (2023). Water, sanitation and hygiene. Accessed on December 2024. Link: <https://www.unicef.org/kenya/water-sanitation-and-hygiene>.
- Usmani, M., Brumfield, K. D., Jamal, Y., Huq, A., Colwell, R. R., and Jutla, A. (2021). A review of the environmental trigger and transmission components for prediction of cholera. *Tropical Medicine and Infectious Disease*, 6(3):147.
- Van den Driessche, P. and Watmough, J. (2002). Reproduction numbers and sub-threshold endemic equilibria for compartmental models of disease transmission. *Mathematical Biosciences*, 180(1-2):29–48.
- Wang, X., Zhao, X.-Q., and Wang, J. (2018). A cholera epidemic model in a spatiotemporally heterogeneous environment. *Journal of Mathematical Analysis and Applications*, 468(2):893–912.
- WHO (2023a). Cholera. Accessed on August 2024. Link: www.who.int/news-room/fact-sheets/detail/cholera.
- WHO (2023b). Disease outbreak. Accessed on December 2024. Link: <https://www.who.int/teams/environment-climate-change-and-health/emergencies/disease-outbreaks#:~:text=%C2%A9,existing%20exposure%20to%20the%20agent>.
- Zheng, Q., Luquero, F. J., Ciglenecki, I., Wamala, J. F., Abubakar, A., Welo, P., Hussen, M., Wossen, M., Yennan, S., Keita, A., et al. (2022). Cholera outbreaks in sub-Saharan Africa during 2010-2019: a descriptive analysis. *International Journal of Infectious Diseases*, 122:215–221.

Appendices

Appendix A: Similarity Report

Patricia_MSc_thesis.pdf

ORIGINALITY REPORT

15%

SIMILARITY INDEX

12%

INTERNET SOURCES

15%

PUBLICATIONS

7%

STUDENT PAPERS

PRIMARY SOURCES

1	www.researchgate.net Internet Source	3%
2	Submitted to Strathmore University Student Paper	2%
3	www.medrxiv.org Internet Source	2%
4	link.springer.com Internet Source	1%
5	Martins O. Onuorah, F. A. Atiku, H. Juuko. "Mathematical model for prevention and control of cholera transmission in a variable population", Research in Mathematics, 2022 Publication	1%
6	Xueying Wang, Xiao-Qiang Zhao, Jin Wang. "A cholera epidemic model in a spatiotemporally heterogeneous environment", Journal of Mathematical Analysis and Applications, 2018 Publication	1%
7	www.hindawi.com Internet Source	1%

8	Abdulrakib Abdulrahim, Ridwan Olamilekan Adesola. "Antimicrobial Resistance in Cholera: A Need for Quick Intervention in Nigeria, West Africa", International Journal of Travel Medicine and Global Health, 2022 Publication	1 %
9	studyres.com Internet Source	1 %
10	scik.org Internet Source	1 %
11	ebin.pub Internet Source	<1 %
12	www.scribd.com Internet Source	<1 %
13	www.researchsquare.com Internet Source	<1 %
14	Submitted to Macquarie University Student Paper	<1 %
15	mdpi-res.com Internet Source	<1 %

Exclude quotes Off
Exclude bibliography On

Exclude matches < 25 words

Appendix B: Ethical Clearance Confirmation



9th December 2024

Ms Charagu Patricia,
patricia.charagu@strathmore.edu

Dear Ms Charagu,

**RE: Modeling Cholera Dynamics in Kenyan Slums: A Comprehensive Analysis
Incorporating WASH Interventions, Vaccination, and Treatment**

This is to inform you that SU-ISERC has reviewed and **approved** your above **SU-masters** proposal. Your application reference number is **SU-ISERC2446/24**. The approval period is from **9th December 2024 to 8th December 2025**.

This approval is subject to compliance with the following requirements:

- i. Only approved documents including (informed consents, study instruments, MTA) will be used.
- ii. All changes including (amendments, deviations, and violations) are submitted for review and approval by SU-ISERC.
- iii. Death and life-threatening problems and serious adverse events or unexpected adverse events whether related or unrelated to the study must be reported to SU-ISERC within 72 hours of notification.
- iv. Any changes anticipated or otherwise that may increase the risks or affected safety or welfare of study participants and others or affect the integrity of the research must be reported to SU-ISERC within 72 hours.
- v. Clearance for the export of biological specimens must be obtained from relevant institutions.
- vi. Submission of a request for renewal of approval at least 60 days prior to the expiry of the approval period. Attach a comprehensive progress report to support the renewal.
- vii. Submission of an executive summary report within 90 days of completion of the study to SU-ISERC.

Before commencing your study, you will be expected to obtain a research license from National Commission for Science, Technology, and Innovation (NACOSTI) <https://research-portal.nacosti.go.ke/> and obtain other clearances needed.

Yours sincerely,

**Mr Ambrose Rachier,
Chairperson; SU-ISERC**

Appendix C: Definitions of Key Terms

Cholera - An acute diarrheal disease that is caused by consumption of food or water contaminated with the bacteria *Vibrio cholerae* (WHO, 2023a).

Control strategies - Deliberate efforts aimed at reducing disease incidence, prevalence, morbidity and mortality to a locally acceptable level (Dowdle, 2023).

Effective reproduction number (R_v) - The average number of secondary cases produced by a single infection in a population where some individuals may not be susceptible (Barratt et al., 2018).

Informal settlements (Slums) - Densely populated urban areas characterized by substandard housing and inadequate access to basic services such as water and sanitation (Citaristi, 2022).

Mathematical modeling - The utilization of mathematical equations and algorithms to simulate and study the behavior of real-world systems, such as the spread of infectious diseases (Brauer et al., 2019).

Outbreak - The occurrence of disease cases in excess of what is normally expected (WHO, 2023b).

Scenario analysis - A method used to evaluate potential outcomes of different scenarios by simulating how changes in key factors might affect a system or process. (Kuddus et al., 2023)

Sensitivity analysis - A method used in modeling to assess how variations in input parameters influence the output (Saltelli et al., 2000).

Susceptible population (S) - The group of individuals who are not immune to a disease and are at risk of infection (Anderson, 2013).

WASH interventions - Programs and practices aimed at improving Water, Sanitation, and Hygiene to prevent the spread of waterborne diseases, including cholera (UNICEF, 2023).

Appendix D: R Codes

```
cholera_model <- function(time, state, parameters) {  
  with(as.list(c(state, parameters)), {  
    N <- S + I_n + T_i + V + R  
    B_effect <- (beta * (1 - omega1) * B) / (K + B)  
    I_n_effect <- (betah * (1 - omega2) * I_n) / N  
    T_i_effect <- (betahT * (1 - omega2) * T_i) / N  
    dS <- pi + theta * V - (B_effect + I_n_effect + T_i_effect) * S - mu1  
    * S - nu * S  
    dI_n <- (B_effect + I_n_effect + T_i_effect) * S - (mu1 + mu2 + gamma  
    + tau) * I_n  
    dT_i <- tau * I_n - (mu1 + mu2 + alpha) * T_i  
    dV <- nu * S - theta * V - mu1 * V  
    dR <- gamma * I_n + alpha * T_i - mu1 * R  
    dB <- epsilont * (1 - omega3) * T_i + epsilon * (1 - omega3)  
    * I_n - delta * (1 + omega4) * B  
    return(list(c(dS, dI_n, dT_i, dV, dR, dB)))  
  })}  
initial_state_values <- c(S = 2700000, I_n = 500000, T_i = 350000,  
V = 600000, R = 0, B = 500)  
times <- seq(0, 1460, 1)  
# Base parameter values  
base_params <- c(pi = 1500, theta = 0.025, beta = 0.214, omega1 = 0.94,  
K = 1e6, betah = 0.02, omega2 = 0.1095, betahT = 0.015, mu1 = 0.0000431,  
nu = 0.004, mu2 = 0.013, gamma = 0.035, tau = 0.3, alpha = 0.0005,  
epsilont = 5, omega3 = 0.94, epsilon = 10, omega4 = 0.73, delta = 0.033)  
# Scenarios for Treated Infected (Ti)  
params_Ti_1 <- base_params # WASH + treatment + vaccination  
params_Ti_1[c("omega1", "omega2", "omega3", "omega4")] <- 0.7
```

```

params_Ti_2 <- base_params # treatment + vaccination
params_Ti_2[c("omega1", "omega2", "omega3", "omega4")] <- 0
params_Ti_3 <- base_params # treatment + WASH
params_Ti_3["nu"] <- 0
params_Ti_3[c("omega1", "omega2", "omega3", "omega4")] <- 0.7
params_Ti_4 <- base_params # treatment alone
params_Ti_4["nu"] <- 0
params_Ti_4[c("omega1", "omega2", "omega3", "omega4")] <- 0
# Scenarios for Untreated Infected (In)
params_In_1 <- base_params # WASH + vaccination
params_In_1["tau"] <- 0
params_In_1[c("omega1", "omega2", "omega3", "omega4")] <- 0.7
params_In_2 <- base_params # WASH alone
params_In_2["nu"] <- 0
params_In_2["tau"] <- 0
params_In_2[c("omega1", "omega2", "omega3", "omega4")] <- 0.7
params_In_3 <- base_params # vaccination alone
params_In_3["tau"] <- 0
params_In_3[c("omega1", "omega2", "omega3", "omega4")] <- 0
output_Ti_1 <- ode(initial_state_values, times, cholera_model, params_Ti_1,
method = "lsoda")
output_Ti_2 <- ode(initial_state_values, times, cholera_model, params_Ti_2,
method = "lsoda")
output_Ti_3 <- ode(initial_state_values, times, cholera_model, params_Ti_3,
method = "lsoda")
output_Ti_4 <- ode(initial_state_values, times, cholera_model, params_Ti_4,
method = "lsoda")
output_In_1 <- ode(initial_state_values, times, cholera_model, params_In_1,
method = "lsoda")
output_In_2 <- ode(initial_state_values, times, cholera_model, params_In_2,

```

```

method = "lsoda")
output_In_3 <- ode(initial_state_values, times, cholera_model, params_In_3,
method = "lsoda")
combined_data_Ti <- rbind(
  data.frame(output_Ti_1, Scenario = "WASH + Treatment + Vaccination"),
  data.frame(output_Ti_2, Scenario = "Treatment + Vaccination"),
  data.frame(output_Ti_3, Scenario = "Treatment + WASH"),
  data.frame(output_Ti_4, Scenario = "Treatment Alone"))
# Combine In data
combined_data_In <- rbind(
  data.frame(output_In_1, Scenario = "WASH + Vaccination"),
  data.frame(output_In_2, Scenario = "WASH Alone"),
  data.frame(output_In_3, Scenario = "Vaccination Alone"))
# Plot for Treated Infected (Ti)
plot_Ti <- ggplot(combined_data_Ti, aes(x = time, y = T_i, color = Scenario))
+ geom_line(linewidth = 0.8) + xlim(0, 300) + ylab("Treated Infected Individuals
(T_i)") + xlab("Time (days)") + theme_bw() + scale_color_manual(values =
c("#E69F00", "#56B4E9", "#009E73", "#999999")) + theme(legend.position = "right",
legend.background = element_rect(fill = "white", color = "black"), panel.grid =
element_blank()) + labs(title = "Impact of Intervention Strategies on T_i")
# Plot for Untreated Infected (In)
plot_In <- ggplot(combined_data_In, aes(x = time, y = I_n, color = Scenario)) +
  geom_line(linewidth = 0.8) + xlim(0, 300) + ylab("Untreated Infected
Individuals (I_n)") + xlab("Time (days)") + theme_bw() + scale_color_manual
(values = c("#E69F00", "#56B4E9", "#009E73")) +
  theme(
    legend.position = "right", # Changed legend position
    legend.background = element_rect(fill = "white", color = "black"),
    panel.grid = element_blank()
  ) + labs(title = "Impact of Intervention Strategies on I_n")

```

Appendix E: Fourth-Order Runge-Kutta (RK4) Algorithm

Consider the initial value problem:

$$\frac{dy}{dt} = f(t, y), \quad y(t_0) = y_0,$$

where $f(t, y)$ is a given function, t_0 is the initial time, and y_0 is the initial value. The RK4 method approximates $y(t)$ at discrete time steps $t_n = t_0 + nh$, where h is the step size. The algorithm proceeds as follows:

1. **Initialize:** Set $t = t_0, y = y_0$.

2. **For each time step:**

$$k_1 = h \cdot f(t, y),$$

$$k_2 = h \cdot f\left(t + \frac{h}{2}, y + \frac{k_1}{2}\right),$$

$$k_3 = h \cdot f\left(t + \frac{h}{2}, y + \frac{k_2}{2}\right),$$

$$k_4 = h \cdot f(t + h, y + k_3).$$

Update the solution:

$$y_{n+1} = y_n + \frac{1}{6}(k_1 + 2k_2 + 2k_3 + k_4),$$

and advance time:

$$t_{n+1} = t_n + h.$$

3. **Repeat** until t reaches the desired endpoint.

Key properties:

- Local truncation error: $\mathcal{O}(h^5)$.
- Global truncation error: $\mathcal{O}(h^4)$.
- The method is explicit and requires four evaluations of $f(t, y)$ per step.